

Effect of Coordination Geometry on Magnetic Properties in a Series of Cobalt(II) Complexes and Structural Transformation in Mother Liquor

*Subrata Ghosh,[†] Sujit Kamilya,[†] Mayurika Das,[†] Sakshi Mehta,[†] Marie-Emmanuelle Boulon,[‡]
Ivan Nemeč,^{§,||} Mathieu Rouzières,[#] Radovan Herchel,[§] and Abhishake Mondal^{*†}*

[†]*Solid State and Structural Chemistry Unit, Indian Institute of Science, Sir C. V. Raman Road, Bangalore 560012, India.*

[‡]*Photon Science Institute, Alan Turing Building, office 3.315, The University of Manchester, Oxford Road, Manchester M13 9PL, United Kingdom.*

[§]*Department of Inorganic Chemistry, Faculty of Science, Palacký University, 17. listopadu 12, CZ-771 46 Olomouc, Czech Republic.*

^{||}*Central European Institute of Technology, CEITEC BUT, Technická 3058/10, 61600, Brno, Czech Republic.*

[#]*Univ. Bordeaux, CNRS, Centre de Recherche Paul Pascal, CRPP, UMR 5031, 33600 Pessac, France.*

Correspondence to: mondal@iisc.ac.in

Table of Content:

Figure S1. Experimental (top) and simulated (bottom) powder XRD pattern of **1**.

Figure S2. Experimental (top) and simulated (bottom) powder XRD pattern of **2**.

Figure S3. Experimental (top) and simulated (bottom) powder XRD pattern of **3**.

Figure S4: TGA plots for **1**, **2** and **3**

Figure S5. A perspective view of a fragment of the supramolecular structure of **3** formed by the N–H···S hydrogen bonds (cyan dotted lines) and weak intermolecular $\pi \cdots \pi$ (red dotted lines). Hydrogen atoms and solvent molecules are omitted for clarity.

Figure S6: ATR spectra of **1**, **2** and **3** at room temperature.

Figure S7. Selected region of the ATR spectra of **1**, **2** and **3** at room temperature.

Figure S8. Solid state UV/vis/NIR spectra of **1**, **2** and **3** in KBr at room temperature.

Figure S9. UV/vis/NIR spectra of **1**, **2** and **3** in DMF at room temperature.

Figure S10. Cyclic voltammogram of **1** in 0.1 M ${}^n\text{Bu}_4\text{NPF}_6/\text{DMF}$ with a scan rate of 0.1 V s⁻¹

Figure S11. Cyclic voltammogram of bbp ligand in 0.1 M ${}^n\text{Bu}_4\text{NPF}_6/\text{DMF}$ with a scan rate of 0.1 V s⁻¹.

Figure S12. Cyclic voltammogram of **2** in 0.1 M ${}^n\text{Bu}_4\text{NPF}_6/\text{DMF}$ with a scan rate of 0.1 V s⁻¹.

Figure S13. Cyclic voltammogram of **3** in 0.1 M ${}^n\text{Bu}_4\text{NPF}_6/\text{DCM}$ with a scan rate of 0.1 V s⁻¹.

Figure S14. Cyclic voltammogram of **3** in 0.1 M ${}^n\text{Bu}_4\text{NPF}_6/\text{DMF}$ with a scan rate of 0.1 V s⁻¹.

Figure S15. Field dependence of the magnetization as M vs H (left) and M vs H/T (right) plots for **1** at 3 and 5 K with sweep-rates of 100 – 600 Oe/min. The solid lines are guide for the eyes.

Figure S16. Field dependence of the magnetization as M vs H (left) and M vs H/T (right) plots for **2** at 2.5, 3, 5 and 8 K. The solid lines are guide for the eyes.

Figure S17. Field dependence of the magnetization as M vs H (left) and M vs H/T (right) plots for **3** at 4 and 6K with sweep-rates of 100 – 600 Oe/min. The solid lines are guide for the eyes.

Figure S18. M vs H plot for **3** at 2 K from -70000 Oe to + 70000 Oe with sweep-rates of 100 – 600 Oe/min. The solid lines are guide for the eyes.

Figure S19. Frequency (1000 Hz) vs temperature plot of the real (χ' , top) and imaginary (χ'' , bottom) components of the ac susceptibility at 0 Oe external dc field and different temperatures from 1.8 – 20 K, respectively with a 3 Oe ac field for a polycrystalline sample of **1**.

Figure S20. Frequency (1000 Hz) vs temperature plot of the real (χ' , top) and imaginary (χ'' , bottom) components of the ac susceptibility at 0 Oe external dc field and different temperatures from 1.8 – 20 K, respectively with a 3 Oe ac field for a polycrystalline sample of **3**.

Figure S21. Frequency dependence of the real (χ' , top) and imaginary (χ'' , bottom) components of the ac susceptibility at different ac frequencies from 1 - 1500 Hz and different external dc field from 500 – 6000 Oe, respectively, with a 3 Oe ac field for a polycrystalline sample of **1** at 1.8 K.

Figure S22. Experimental Cole-Cole Plots with generalized Debye fit of **2** at 2 K at different DC field.

Figure S23. Field dependence of the parameters, α , ν , χ_0 and χ_∞ between 0 and 1 T deduced from the generalized Debye fit of the frequency dependence of the real (χ') and imaginary (χ'') components of the ac susceptibility at 2 K, for a polycrystalline sample of **2**.

Figure S24. Experimental Cole-Cole Plots with generalized Debye fit of **2** at 1000 Oe DC field at different temperatures.

Figure S25. Temperature dependence of the parameters, α , ν , χ_0 and χ_∞ between 1.9 and 8 K deduced from the generalized Debye fit of the frequency dependence of the real (χ') and imaginary (χ'') components of the ac susceptibility at 1000 Oe, for a polycrystalline sample of **2**.

Figure S26. Frequency dependence of the real (χ' , left) and imaginary (χ'' , right) components of the ac susceptibility at different ac frequencies from 1 - 1500 Hz and different external dc field from 500 – 6000 Oe, respectively with a 3 Oe ac field for a polycrystalline sample of **3** at 1.8 K.

Figure S27. Field dependence of the characteristic relaxation frequency for **3** at 2 K.

Figure S28. Frequency dependence of the real (χ' , top) and imaginary (χ'' , bottom) components of the ac susceptibility at different temperatures from 1.8 - 10 K and different ac frequencies from 1 - 1500 Hz, respectively, with a 3 Oe ac field for a polycrystalline sample of **3** at 1500 Oe external dc field.

Figure S29. Experimental Cole-Cole Plots without fit (left) and with generalized Debye fit (right) of **3** at 1500 Oe DC field at different temperatures.

Figure S30. DSC plot of **1** from 295 – 130 K (left) and 295 – 372 K (right) at cooling/heating rates of 5 K/ min. The heating and cooling modes are in red and blue lines, respectively.

Figure S31. DSC plot of **2** from 295 – 130 K at cooling/heating rates of 5 K/ min. The heating and cooling modes are in red and blue lines, respectively.

Figure S32. DSC plot of **3** from 295 – 130 K at cooling/heating rates of 5 K/ min. The heating and cooling modes are in red and blue lines, respectively.

Figure S33. The X-band EPR data for **1** at $T = 5$ K. The calculated data corresponds to two Kramers doublets with $S_{\text{eff}} = 1/2$, first doublet with $g_{xy} = 4.781$, $g_z = 1.927$, linewidth = 58.5 mT; second doublet with $g_{xy} = 3.359$, $g_z = 2.148$, linewidth = 16.3 mT, where weight ratio between these two doublets are 1: 0.0496, respectively.

Figure S34. The X-band EPR data for **3** at $T = 5$ K. The calculated data corresponds to Kramers doublet with $S_{\text{eff}} = 1/2$ using $g_x = 5.669$, $g_y = 4.169$, $g_z = 1.954$, and H-strain defined as (2742, 3360, 1801) MHz.

Figure S35. The multiplet energy levels calculated by CASSCF/NEVPT2 for [Co(bbp)(NCS)₂(DMF)] complex of **2** (black) and reconstructed energy levels with Figgis-Griffith Hamiltonian (eq.5) (red) using following parameters: $\alpha \lambda = -245 \text{ cm}^{-1}$, $\Delta_{\text{ax}} = -714 \text{ cm}^{-1}$, $\Delta_{\text{rh}} = -151 \text{ cm}^{-1}$.

Figure S36. The magnetic data for **2**. The empty symbols – experimental data, full lines – calculated data using L-S Hamiltonian with parameters in text.

Table S1. Selected bond lengths (Å) and bond angles (°) in **1** (120 K), **2** (293 K) and **3** (120 K).

Table S2. CShM analysis data for complexes **1**, **2** and **3**.

Table S3. Short intra- and inter molecular interactions in **1**, **2** and **3**.

Table S4. Cole-Cole parameters for complex **2** at 1000 Oe

Table S5. Cole-Cole parameters for complex **3** at 1500 Oe

Table S6. Magnetic anisotropy and SMM parameters for mononuclear Co(II) hexa-, penta- and tetra coordinated complexes

Appendix: Check cif files for complexes **1**, **2** and **3**.

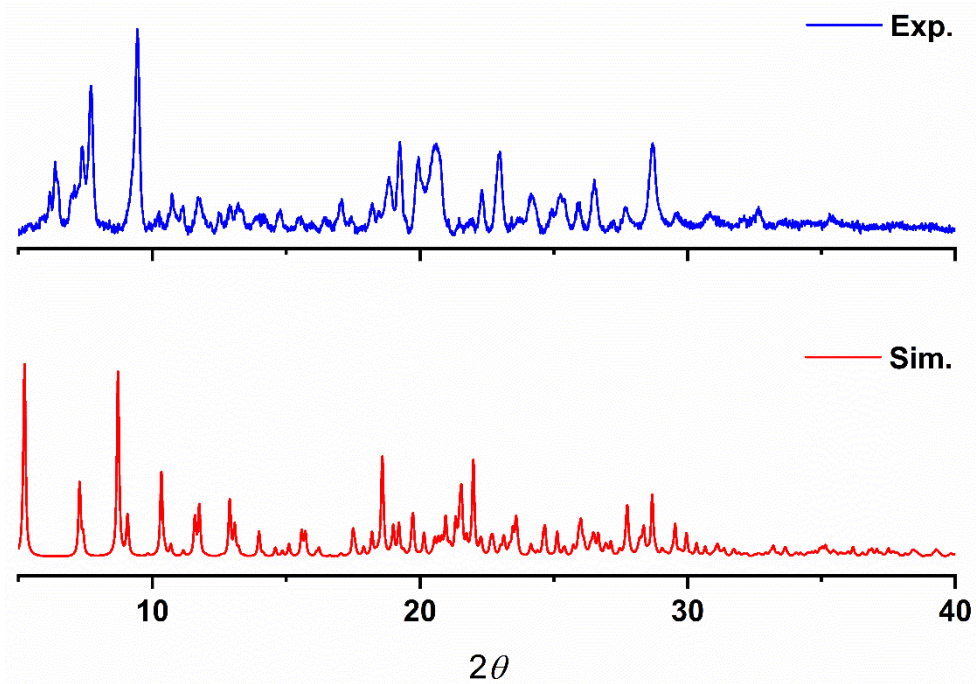


Figure S1. Experimental (top) and simulated (bottom) powder XRD pattern of 1.

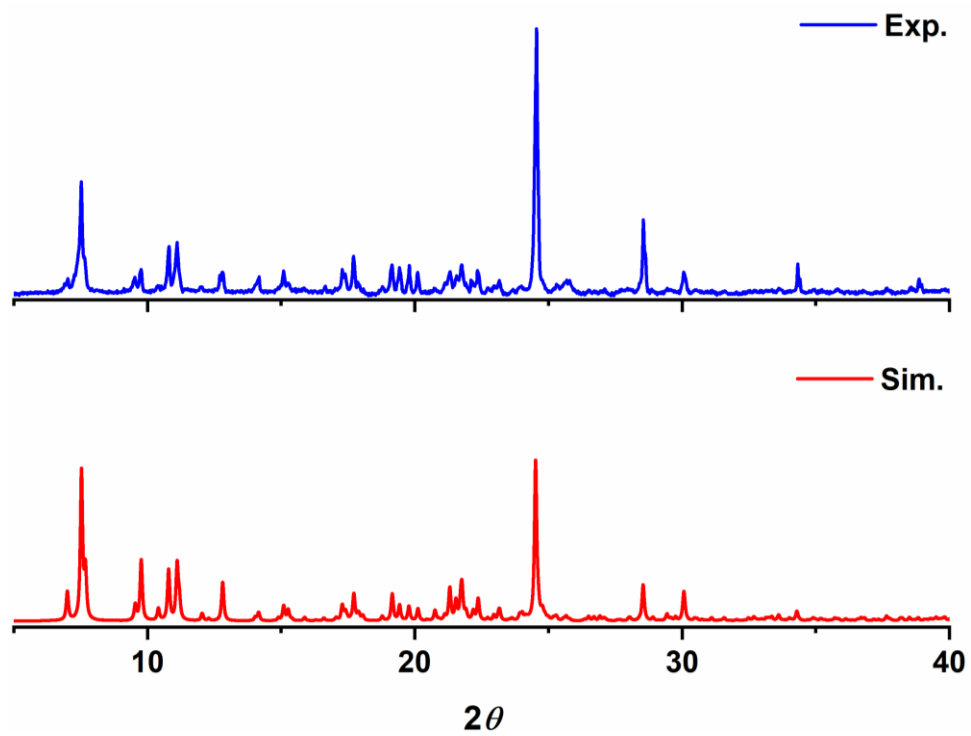


Figure S2. Experimental (top) and simulated (bottom) powder XRD pattern of 2.

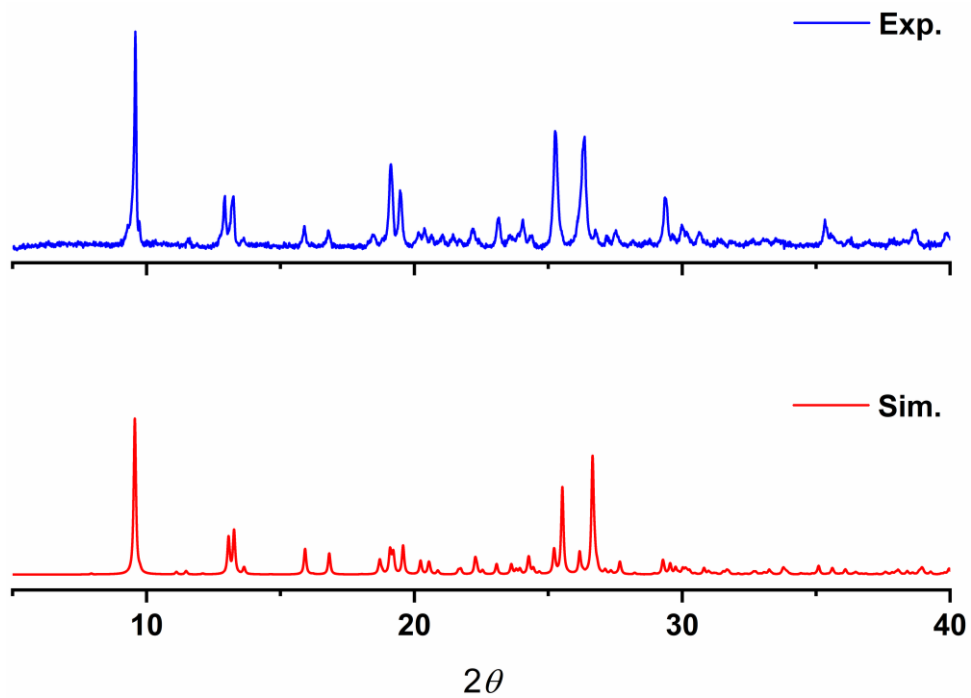


Figure S3. Experimental (top) and simulated (bottom) powder XRD pattern of 3.

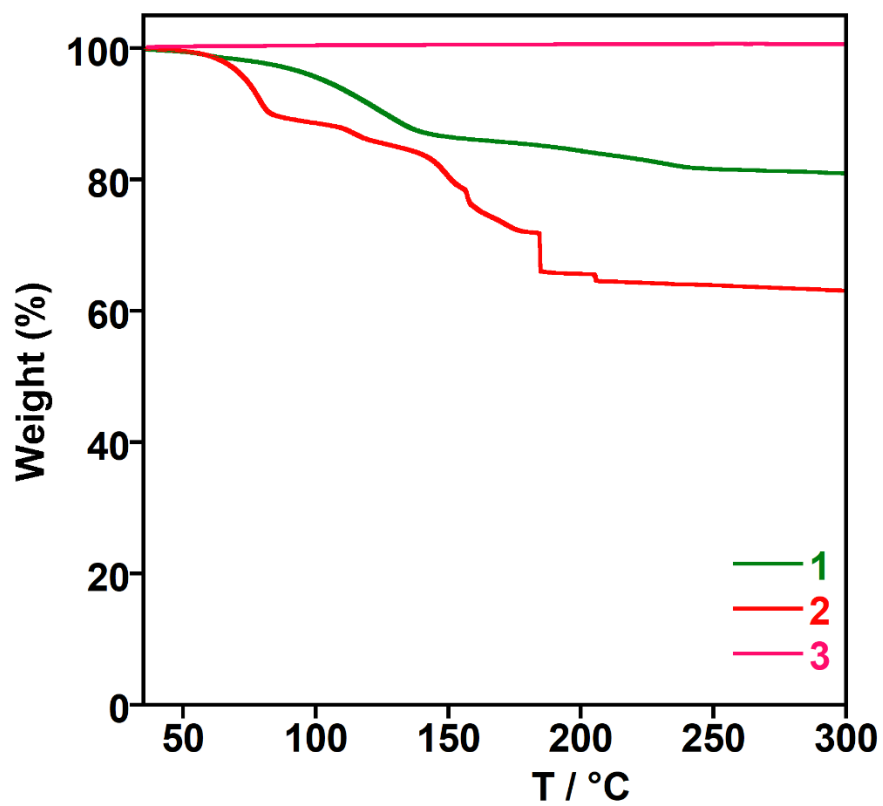


Figure S4: TGA plots for 1, 2 and 3

Table S1. Selected bond lengths (Å) and bond angles (°) in **1** (120 K), **2** (293 K) and **3** (120 K).

1		2		3	
Co(1)-N(1)	2.175(3)	Co(1)-N(1)	2.167(3)	Co(1)-N(1)	2.122(2)
Co(1)-N(3)	2.090(4)	Co(1)-N(3)	2.111(2)	Co(1)-N(3)	2.086(2)
Co(1)-N(4)	2.177(3)	Co(1)-N(4)	2.164(3)	Co(1)-N(4)	2.172(2)
Co(1)-N(6)	2.140(3)	Co(1)-N(6)	2.022(4)	Co(1)-N(6)	1.976(2)
Co(1)-N(8)	2.092(3)	Co(1)-N(7)	2.079(3)	Co(1)-N(7)	1.982(3)
Co(1)-N(9)	2.162(3)	Co(1)-O(1)	2.272(2)	N(1)-Co(1)-N(3)	76.63(8)
Co(2)-N(11)	1.953(7)	N(1)-Co(1)-N(3)	75.5(1)	N(1)-Co(1)-N(4)	151.34(9)
Co(2)-N(12)	1.942(8)	N(1)-Co(1)-N(4)	150.5(1)	N(1)-Co(1)-N(6)	106.1(1)
Co(2)-N(13)	1.947(5)	N(1)-Co(1)-N(6)	101.7(1)	N(1)-Co(1)-N(7)	97.6(1)
Co(2)-N(14)	1.943(5)	N(1)-Co(1)-N(7)	91.5(1)	N(3)-Co(1)-N(4)	75.09(8)
N(1)-Co(1)-N(3)	75.7(1)	N(1)-Co(1)-O(1)	89.1(1)	N(3)-Co(1)-N(6)	116.3(1)
N(1)-Co(1)-N(4)	151.6(1)	N(3)-Co(1)-O(1)	87.09(9)	N(3)-Co(1)-N(7)	134.3(1)
N(1)-Co(1)-N(6)	89.4(1)	N(4)-Co(1)-O(1)	84.9(1)	N(4)-Co(1)-N(6)	90.5(1)
N(1)-Co(1)-N(8)	116.2(1)	N(6)-Co(1)-O(1)	87.8(1)	N(4)-Co(1)-N(7)	98.8(1)
N(1)-Co(1)-N(9)	96.9(1)	N(7)-Co(1)-O(1)	174.3(1)	N(6)-Co(1)-N(7)	108.9(1)
N(3)-Co(1)-N(4)	76.1(1)	Co(1)-N(6)-C(21)	172.9(4)	Co(1)-N(6)-C(20)	162.6(3)
N(3)-Co(1)-N(6)	106.2(1)	Co(1)-N(7)-C(20)	142.8(3)	Co(1)-N(7)-C(21)	161.9(3)
N(3)-Co(1)-N(8)	168.1(1)	Co(1)-O(1)-C(22)	116.4(2)	N(6)-C(20)-S(2)	177.2(3)
N(3)-Co(1)-N(9)	103.1(1)	N(6)-C(21)-S(2)	179.3(4)	N(7)-C(21)-S(1)	177.8(3)
N(4)-Co(1)-N(6)	95.4(1)	N(7)-C(20)-S(1)	178.1(4)		
N(4)-Co(1)-N(8)	92.1(1)				
N(4)-Co(1)-N(9)	92.5(1)				
N(6)-Co(1)-N(8)	75.9(1)				
N(6)-Co(1)-N(9)	150.7(1)				
N(8)-Co(1)-N(9)	75.7(1)				
N(11)-Co(2)-N(12)	112.1(3)				
N(11)-Co(2)-N(13)	109.8(2)				
N(11)-Co(2)-N(14)	108.4(2)				
N(12)-Co(2)-N(13)	107.0(3)				
N(12)-Co(2)-N(14)	112.1(3)				
N(13)-Co(2)-N(14)	107.3(2)				
Co(2)-N(11)-C(39)	172.8(6)				
Co(2)-N(12)-C(40)	166.4(9)				
Co(2)-N(13)-C(41)	174.3(5)				
Co(2)-N(14)-C(42)	168.4(5)				
N(11)-C(39)-S(1)	179.2(7)				
N(12)-C(40)-S(2)	178(1)				
N(13)-C(41)-S(3)	177.9(6)				
N(14)-C(42)-S(4)	179.2(5)				

Continuous Shape Measures (CShM) Analysis:

Continuous Shape Measures (CShM) analysis was carried out to determine the geometry around Co atom. Based on the values obtained, the idealized polyhedron was matched with the actual coordination spheres. The smallest value is symbolic of proximity of actual coordination sphere and idealized polyhedron.

Table S2. CShM analysis data for complexes **1**, **2** and **3**.

Complex 1	Structure				
	HP - 6	PPY - 6	OC - 6	TPR - 6	JPPY - 6
$[\text{Co}(\text{bbp})_2]^{2+}$	32.849	18.114	4.718	9.304	22.122
	SP - 4	T - 4	SS - 4	vTBPY - 4	
$[\text{Co}(\text{NCS})_4]^{2-}$	32.126	0.053	9.054	3.091	
Complex 2	Structure				
	HP - 6	PPY - 6	OC - 6	TPR - 6	JPPY - 6
$[\text{Co}(\text{bbp})(\text{NCS})_2(\text{DMF})]$	32.429	24.111	1.398	14.459	28.704
Complex 3	Structure				
	PP - 5	VOC - 5	TBPY - 5	SPY - 5	JTBPY - 5
$[\text{Co}(\text{bbp})(\text{NCS})_2]$	27.190	4.558	2.941	2.855	5.172

HP – 6: Hexagon (D_{6h}), PPY – 6 = Pentagonal pyramid, OC – 6: Octahedron (O_h), TPR – 6: Trigonal prism (D_{3h}), JPPY – 6 = Johnson pentagonal pyramid J₂ (C_{5v}); SP – 4: Square (D_{4h}), T – 4: Tetrahedron (T_d), SS – 4: Seesaw (C_{2v}), vTBPY – 4= Vacant trigonal bipyramid (C_{3v}); PP – 5 = Pentagon (D_{5h}), vOC – 5: Vacant octahedron (C_{4v}), TBPY – 5 = Trigonal bipyramid (D_{3h}), SPY-5 : Spherical square pyramid (C_{4v}), JTBPY – 5 = Johnson trigonal bipyramid J₁₂ (D_{3h}).

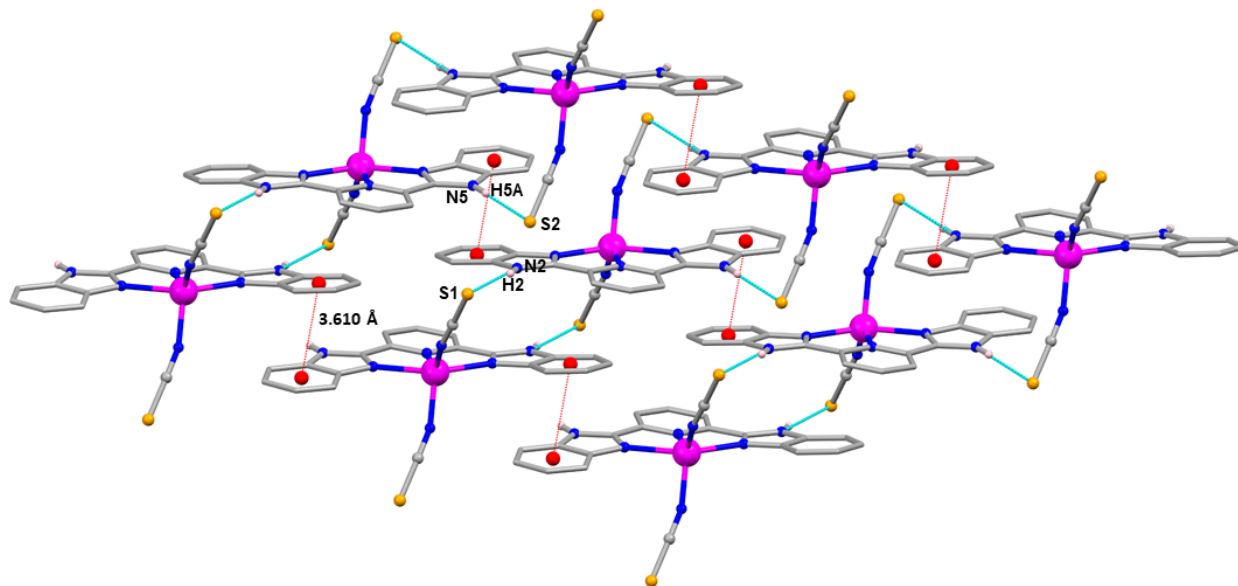


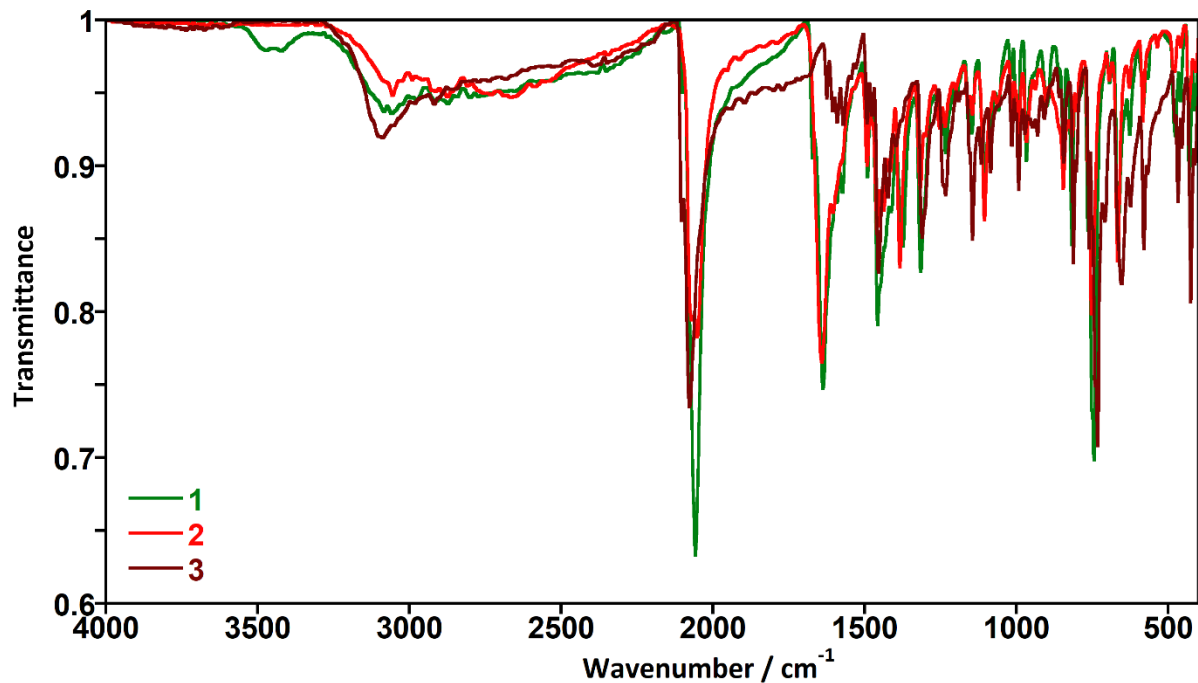
Figure S5. A perspective view of a fragment of the supramolecular structure of **3** formed by the N–H···S hydrogen bonds (cyan dotted lines) and weak intermolecular π ··· π (red dotted lines). Hydrogen atoms and solvent molecules are omitted for clarity.

Table S3. Short intra- and inter molecular interactions in **1**, **2** and **3**.

	D-H...A	D-H / Å	H...A / Å	D...A / Å	∠D-H...A
1	N2-H2A...O1	0.88	1.903	2.767(5)	167.0
	N5-H5A...O3	0.88	1.794	2.673(7)	175.1
	N10-H10A...O4	0.88	1.853	2.729(4)	165.6
	N7-H7A...O2	0.88	1.884	2.745(5)	172.9
2	N2-H2A...O3	0.84	1.91(5)	2.746(5)	176.15°
	N5-H5A...O2	0.91	1.81(5)	2.712(5)	178.29°
	C27-H27...N7	0.96	2.727(5)	3.636(7)	157.47°
	C25-H25B...C21	0.96	2.882(2)	3.428(6)	117.15°
	C24-H24B...C21	0.96	2.767(2)	3.557(6)	140.16°
3	N2-H2...S1	0.88	2.442	3.271(2)	157.2
	N5-H5A...S2	0.88	2.448	3.313(2)	167.4

IR Spectroscopic studies:

Complexes **1**, **2** and **3** were characterized by solid state IR spectroscopy at room temperature (Figures S6 and S7). Complex **1** exhibits peaks at 2100 and 2059 cm^{-1} which correspond to the characteristic $\text{N}\equiv\text{C}$ stretching vibration of NCS^- anions of $[\text{Co}(\text{NCS})_4]^{2-}$ unit, whereas complex **2** shows the $\text{N}\equiv\text{C}$ stretching frequency of NCS^- at 2073 and 2052 cm^{-1} . In addition, both complexes also show $\text{C}=\text{O}$ stretching vibration of DMF molecule at around 1638 cm^{-1} . Complex **3** exhibits peaks at 2103 and 2077 cm^{-1} for $\text{N}\equiv\text{C}$ stretching from NCS^- . Moreover, all complexes display typical absorption of coordinated bbp ligand at around 1591, 1571, 1454, 1312, 1234, 1075, 995 and 583 cm^{-1} .

**Figure S6:** ATR spectra of **1**, **2** and **3** at room temperature.

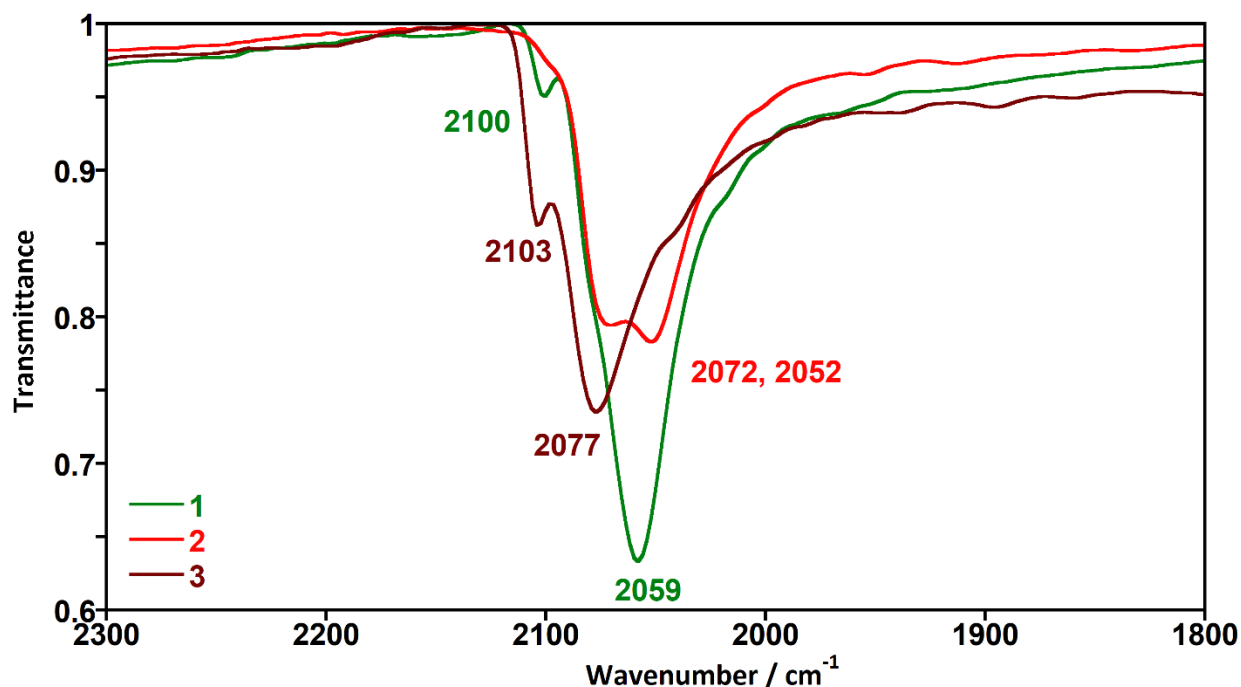


Figure S7. Selected region of the ATR spectra of **1**, **2** and **3** at room temperature.

UV/vis/NIR spectroscopic studies:

UV/vis/NIR studies were carried out on complexes **1**, **2** and **3** in solid state as well as in solution at room temperature (Figures S8 and S9). UV/vis/NIR spectrum of the complex **1** in DMF shows a broad band at 7980 cm⁻¹ and a sharp band at 16000 cm⁻¹ which correspond to d-d transitions ${}^4T_{1g} \rightarrow {}^4T_{2g}({}^4F)$ from HS $[\text{Co}(\text{bbp})_2]^{2+}$ unit and ${}^4A_2 \rightarrow {}^4T_1({}^4P)$ from $[\text{Co}(\text{NCS})_4]^{2-}$ unit respectively). In addition, the complex exhibits ligand based intra ligand charge transfer (ILCT) transition at 30750 cm⁻¹ coming from bbp ligand. The solid-state spectrum of **1** shows very similar absorption bands. The comparison with the solution spectrum suggested that the complex preserved its identity upon dissolution. Solid state UV/vis/NIR spectrum of the complex **2** exhibits two broad bands and a shoulder at around 8070, 17050 and 17780 cm⁻¹ respectively which are attributed to d-d transitions (${}^4T_{1g} \rightarrow {}^4T_{2g}({}^4F)$, ${}^4T_{1g} \rightarrow {}^4A_{2g}({}^4F)$ and ${}^4T_{1g} \rightarrow {}^4T_{1g}({}^4P)$) from HS Co(II) ion with LMCT transitions at around 20400 and 21600 cm⁻¹. It is worth mentioning that the UV/vis/NIR spectrum of **2** in DMF is very similar to that of **1**, which suggested that complex **2** is not stable in DMF solution (one possible explanation: complex **2** in solution is converting to **1**). Solid state spectrum of **3** shows characteristic d-d transitions for HS Co(II) ion in distorted square pyramidal system at around 17200, 15400, 12500 and 9830 cm⁻¹ with ILCT (24800 cm⁻¹) and LMCT (21600 and 20400 cm⁻¹) transitions. However, solution spectrum of **3** in DMF is completely different from solid state and rather similar to the spectrum of **1**, suggested that complex **3** is not stable in DMF solution and converting to **1** from TBP geometry.

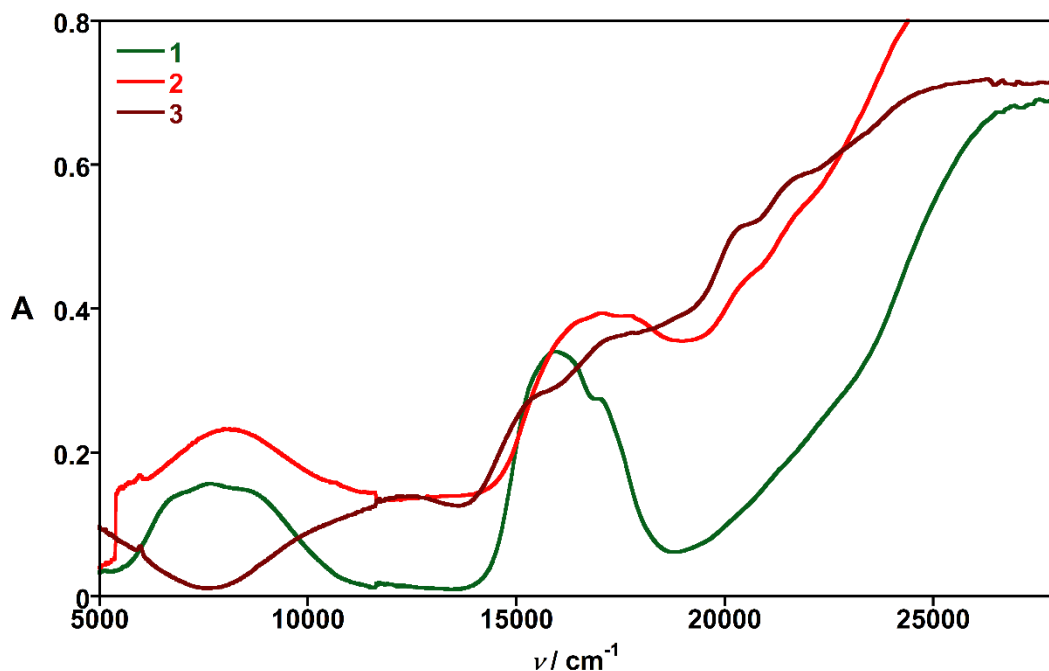


Figure S8. Solid state UV/vis/NIR spectra of **1**, **2** and **3** in KBr at room temperature.

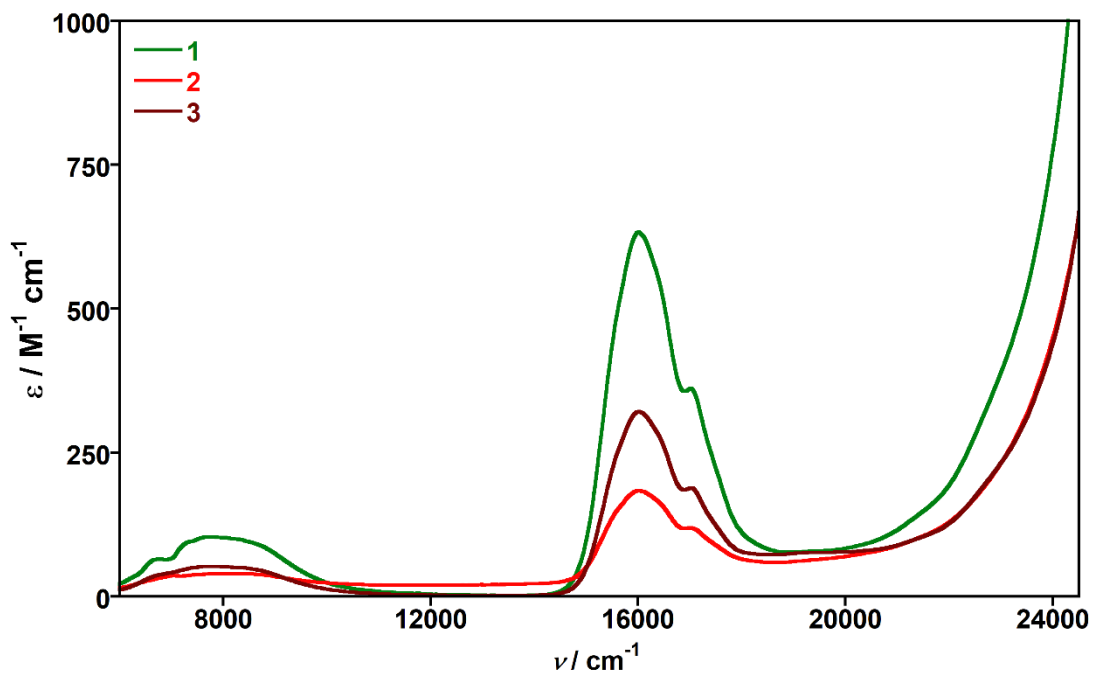


Figure S9. UV/vis/NIR spectra of **1**, **2** and **3** in DMF at room temperature.

Electrochemical studies.

Electrochemical properties of bbp ligand, **1**, **2** and **3** were investigated by cyclic voltammetry in DMF or DCM solution containing ${}^n\text{Bu}_4\text{NPF}_6$ as electrolyte (Figure S10 – S14). Cyclic voltammogram of bbp ligand in DMF shows an irreversible reduction at -1.73 V vs Fc/Fc^+ . Cyclic voltammogram of **1** in DMF displays

two quasireversible oxidation for each Co(II) center of $[\text{Co}(\text{bbp})_2]^{2+}$ unit and $[\text{Co}(\text{NCS})_4]^{2-}$ unit at $-0.05 \text{ V vs Fc/Fc}^+$ ($E_{\text{pa}} = 0.03 \text{ V}$ and $E_{\text{pc}} = -0.07 \text{ V}$) and $0.59 \text{ V vs Fc/Fc}^+$ ($E_{\text{pa}} = 0.75 \text{ V}$ and $E_{\text{pc}} = 0.43 \text{ V}$) which is very close to the previously reported value. Apart from the oxidation, the cyclic voltammogram of **1** also reveals a quasireversible reduction processes at $-0.88 \text{ V vs Fc/Fc}^+$ ($E_{\text{pc}} = -0.99 \text{ V}$ and $E_{\text{pa}} = -0.77 \text{ V}$) which corresponds to reduction of Co(II) center of $[\text{Co}(\text{bbp})_2]^{2+}$ unit. In addition, complex **1** show coordinated bbp ligand-based reduction at $-1.27, -1.45$ and $-1.73 \text{ V vs Fc/Fc}^+$. As shown in Figure S11, cyclic voltammogram of **2** in DMF displays similar feature as that of **1**. Complex **3** in DCM exhibits a quasireversible oxidation for Co(II) center at $0.29 \text{ V vs Fc/Fc}^+$ ($E_{\text{pa}} = 0.50 \text{ V}$ and $E_{\text{pc}} = 0.08 \text{ V}$). However, cyclic voltammogram of **3** in DMF shows similar behavior as that of **1**.

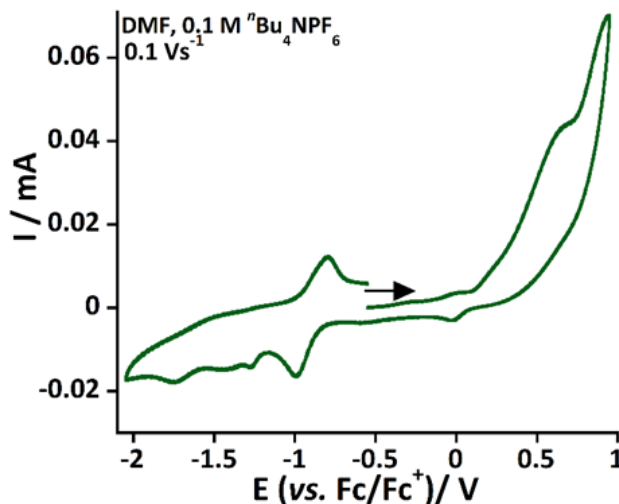


Figure S10. Cyclic voltammogram of **1** in $0.1 \text{ M } n\text{Bu}_4\text{NPF}_6/\text{DMF}$ with a scan rate of 0.1 V s^{-1}

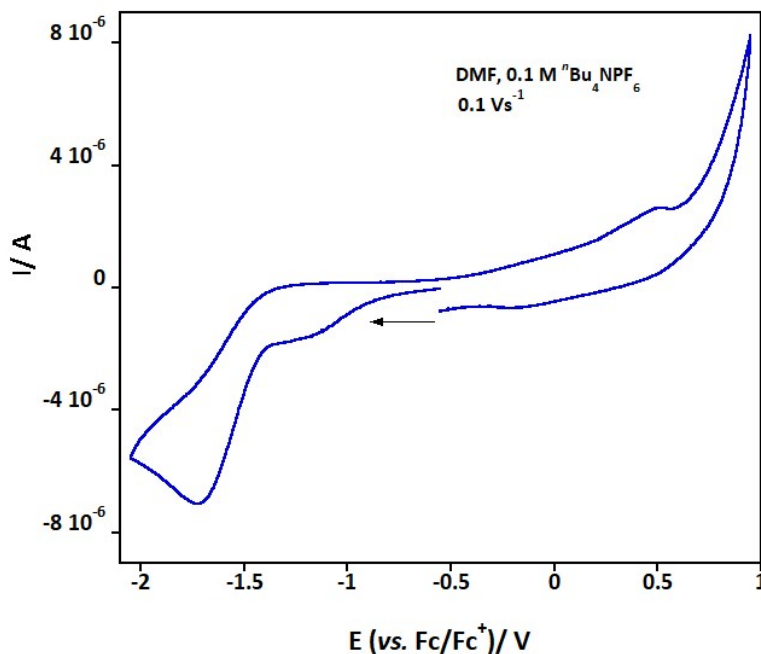


Figure S11. Cyclic voltammogram of bbp ligand in $0.1 \text{ M } n\text{Bu}_4\text{NPF}_6/\text{DMF}$ with a scan rate of 0.1 V s^{-1} .

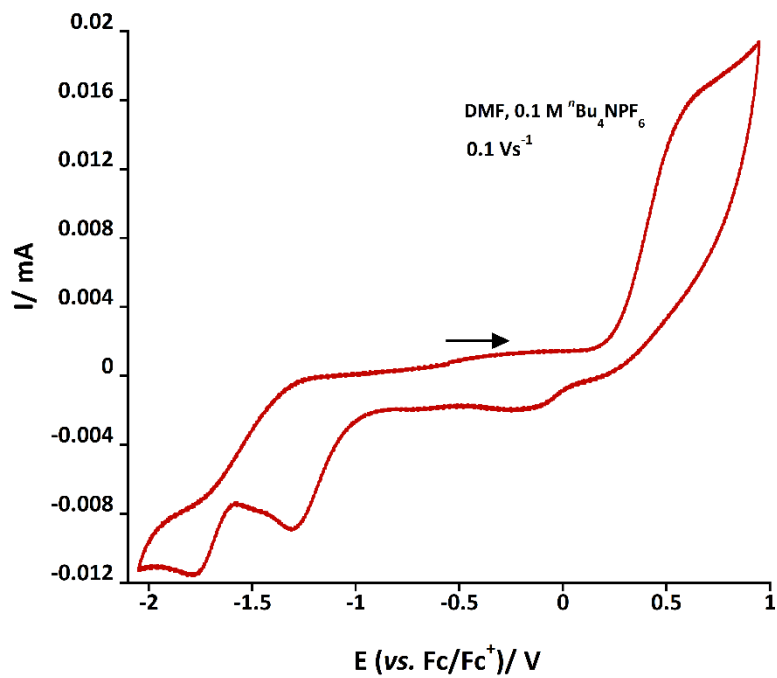


Figure S12. Cyclic voltammogram of **2** in 0.1 M $t\text{Bu}_4\text{NPF}_6/\text{DMF}$ with a scan rate of 0.1 V s^{-1} .

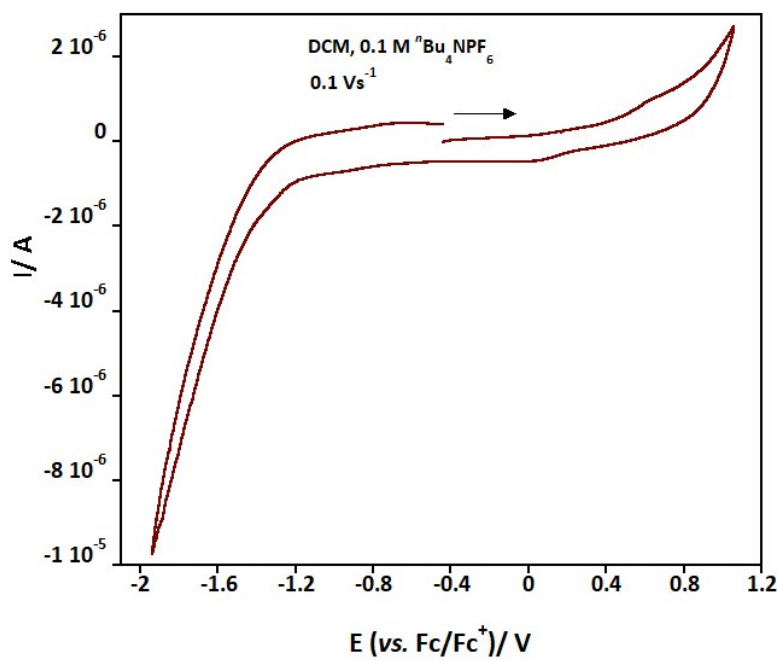


Figure S13. Cyclic voltammogram of **3** in 0.1 M $t\text{Bu}_4\text{NPF}_6/\text{DCM}$ with a scan rate of 0.1 V s^{-1} .

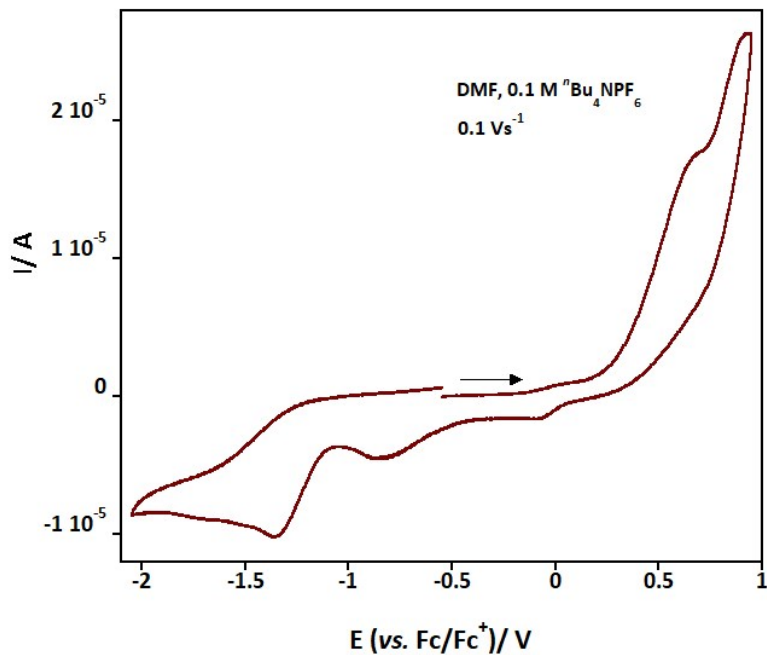


Figure S14. Cyclic voltammogram of **3** in 0.1 M $t\text{Bu}_4\text{NPF}_6/\text{DMF}$ with a scan rate of 0.1 V s^{-1} .

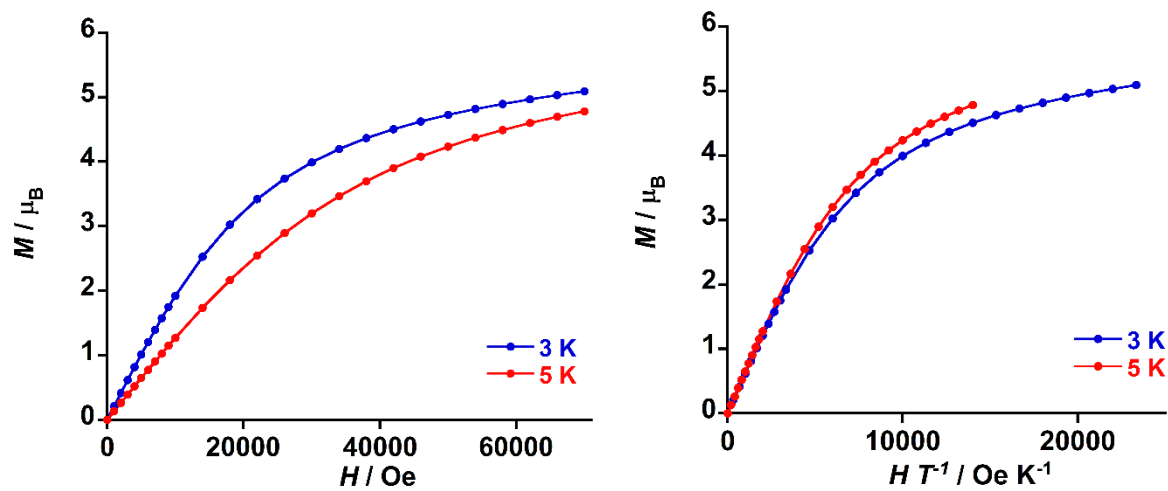


Figure S15. Field dependence of the magnetization as M vs H (left) and M vs H/T (right) plots for **1** at 3 and 5 K with sweep-rates of 100 – 600 Oe/min. The solid lines are guide for the eyes.

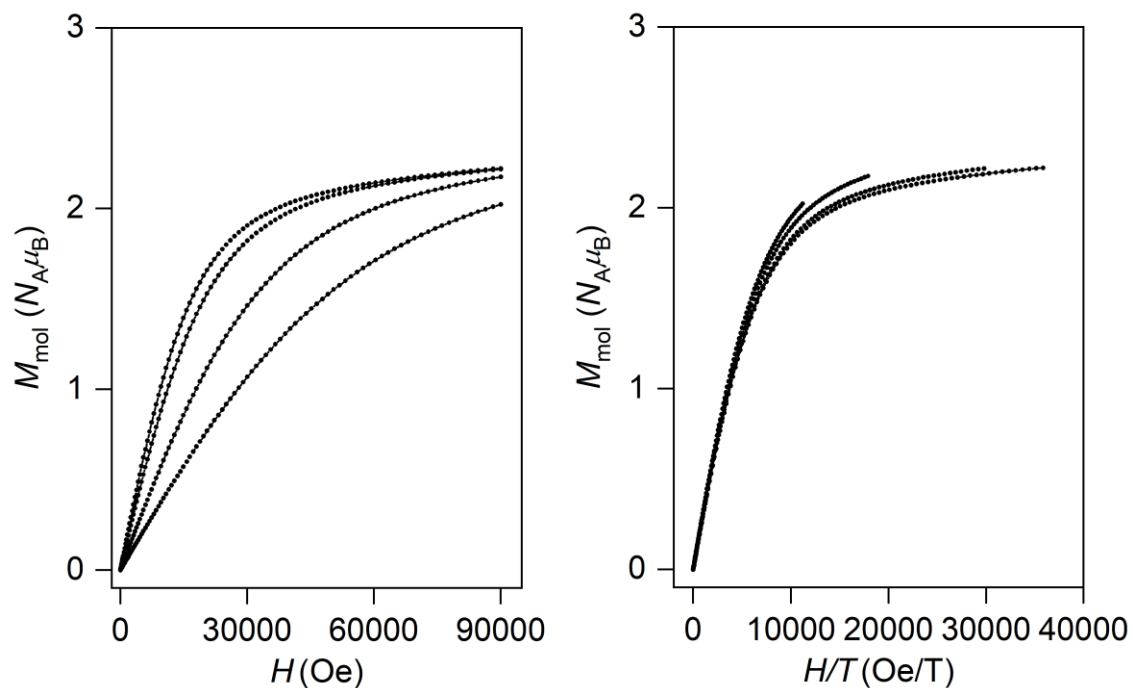


Figure S16. Field dependence of the magnetization as M vs H (left) and M vs H/T (right) plots for **2** at 2.5, 3, 5 and 8 K. The solid lines are guide for the eyes.

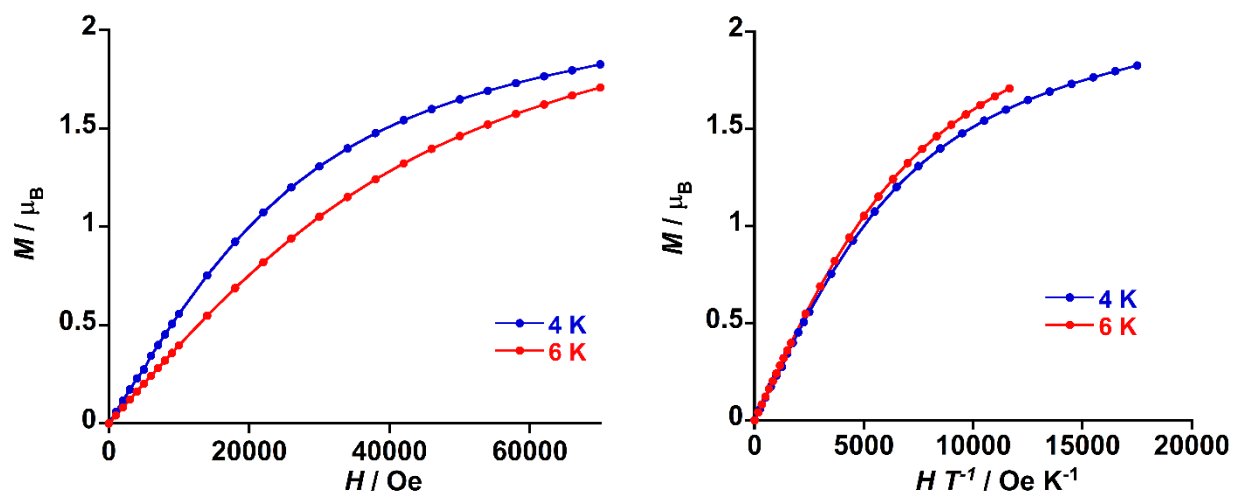


Figure S17. Field dependence of the magnetization as M vs H (left) and M vs H/T (right) plots for **3** at 4 and 6 K with sweep-rates of 100 – 600 Oe/min. The solid lines are guide for the eyes.

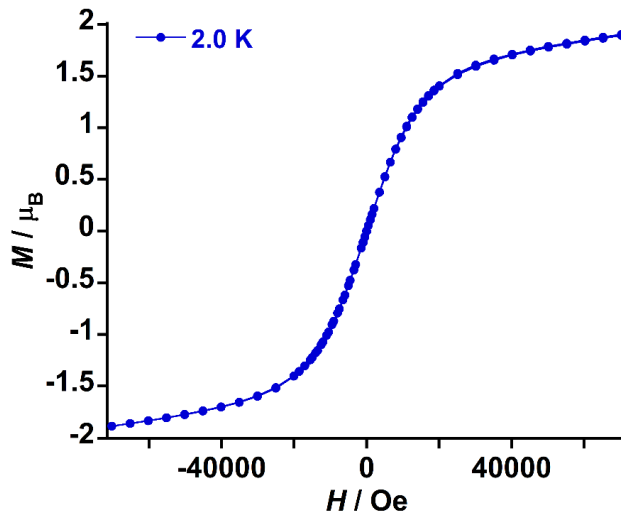


Figure S18. M vs H plot for **3** at 2 K from -70000 Oe to +70000 Oe with sweep-rates of 100 – 600 Oe/min. The solid lines are guide for the eyes.

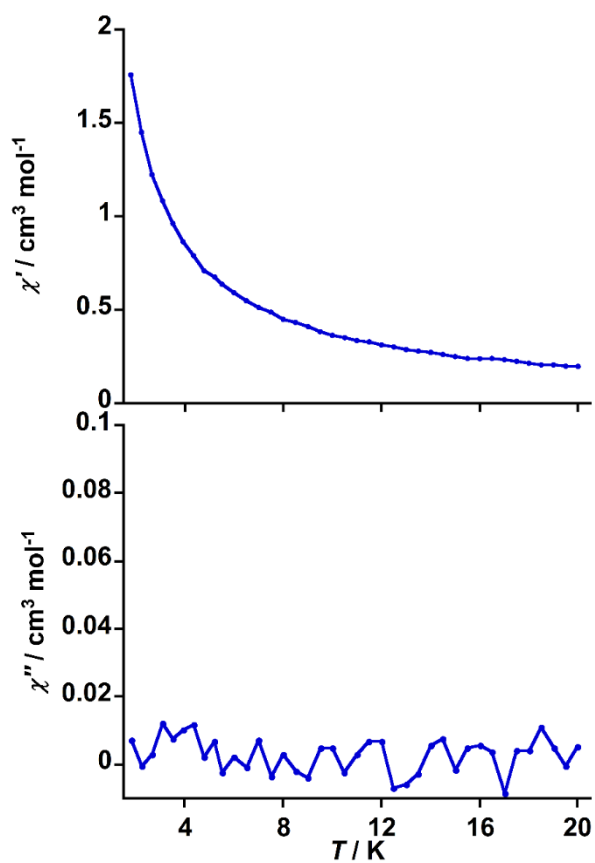


Figure S19. Frequency (1000 Hz) vs temperature plot of the real (χ' , top) and imaginary (χ'' , bottom) components of the ac susceptibility at 0 Oe external dc field and different temperatures from 1.8 – 20 K, respectively with a 3 Oe ac field for a polycrystalline sample of **1**.

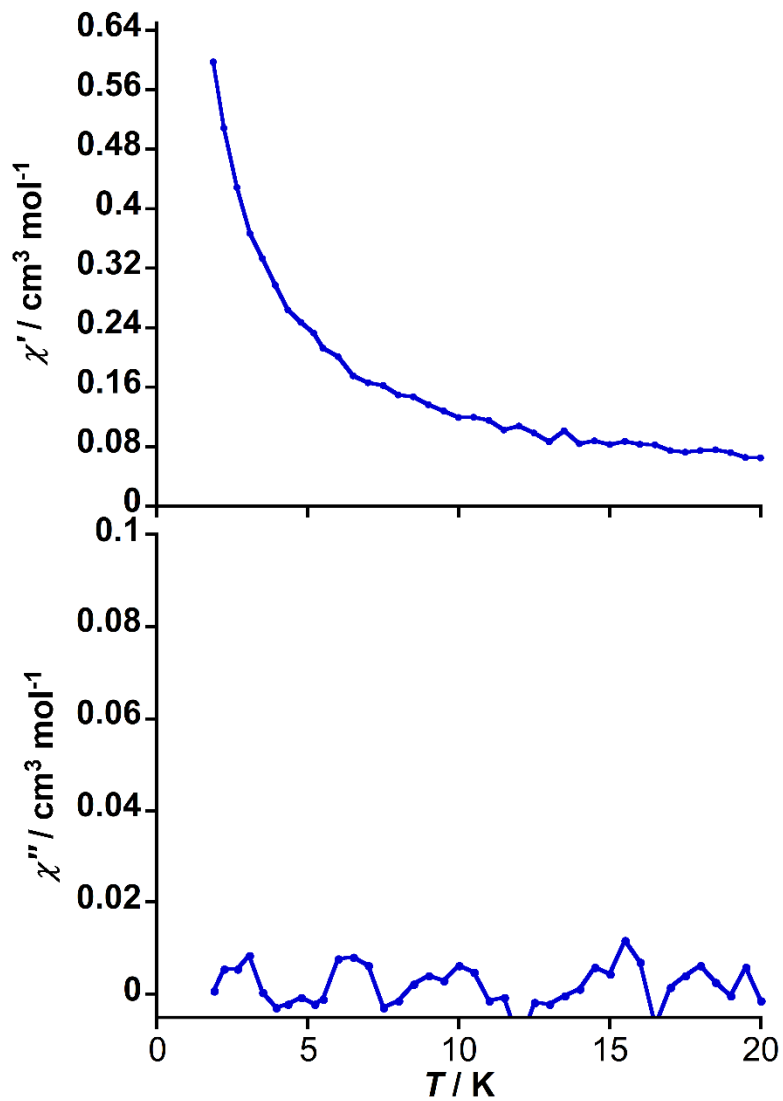


Figure S20. Frequency (1000 Hz) vs temperature plot of the real (χ' , top) and imaginary (χ'' , bottom) components of the ac susceptibility at 0 Oe external dc field and different temperatures from 1.8 – 20 K, respectively with a 3 Oe ac field for a polycrystalline sample of **3**.

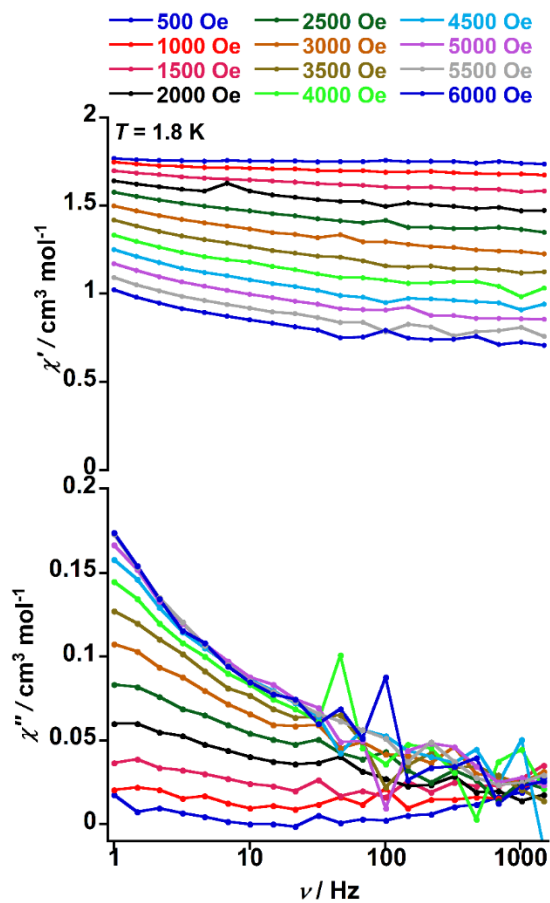


Figure S21. Frequency dependence of the real (χ' , top) and imaginary (χ'' , bottom) components of the ac susceptibility at different ac frequencies from 1 - 1500 Hz and different external dc field from 500 – 6000 Oe, respectively, with a 3 Oe ac field for a polycrystalline sample of **1** at 1.8 K.

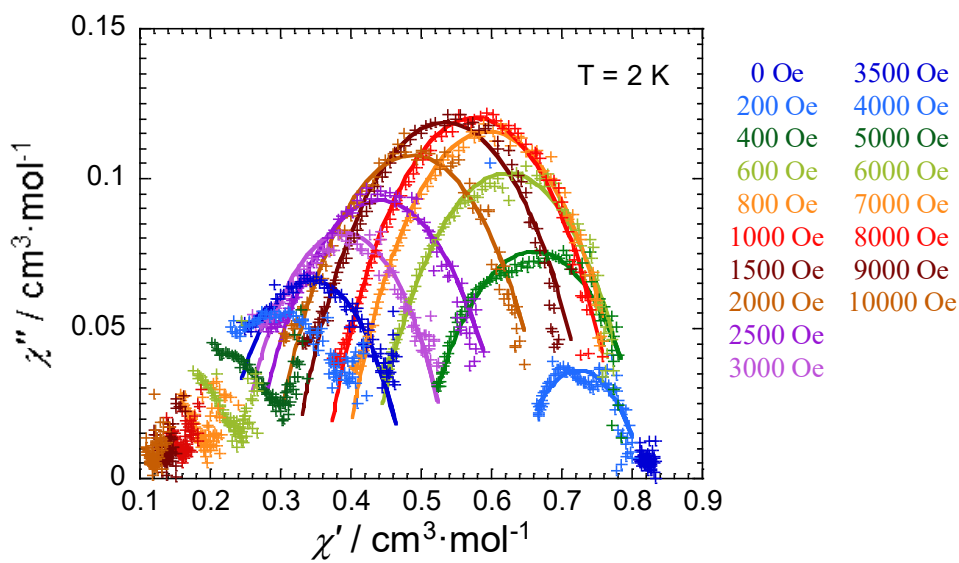


Figure S22. Experimental Cole-Cole Plots with generalized Debye fit of **2** at 2 K at different DC field.

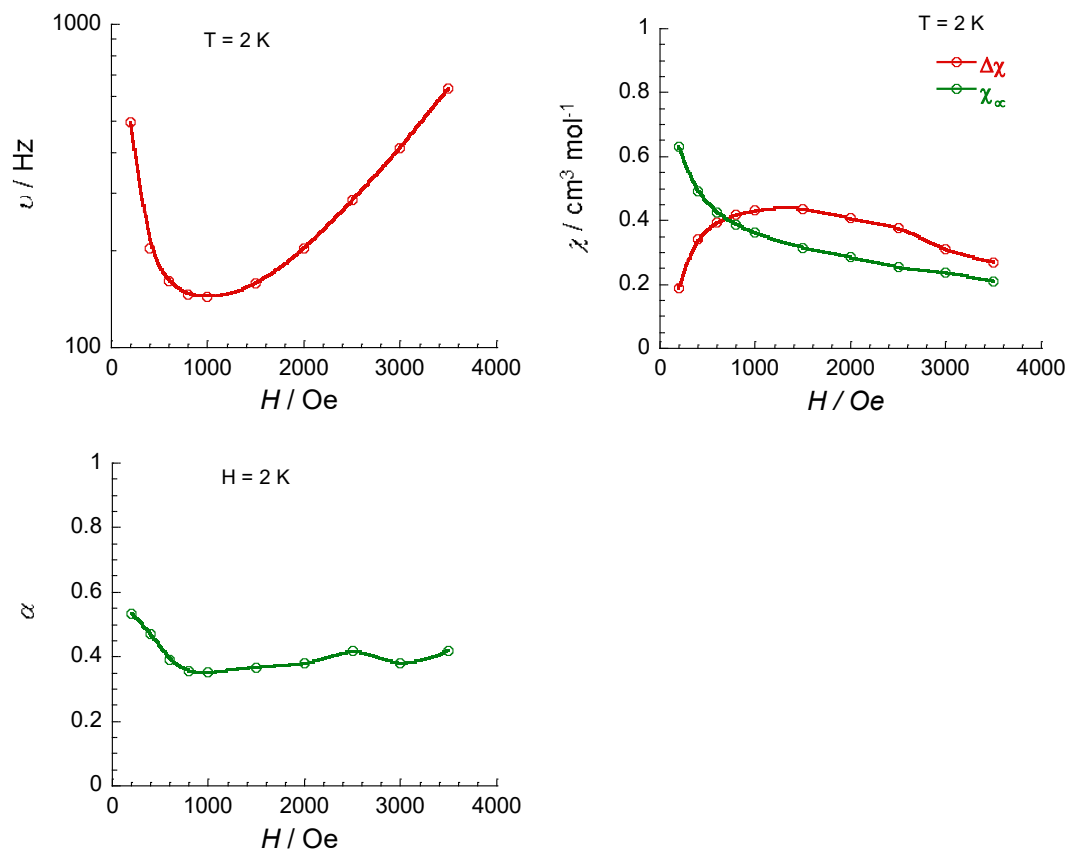


Figure S23. Field dependence of the parameters, α , ν , χ_0 and χ_∞ between 0 and 1 T deduced from the generalized Debye fit of the frequency dependence of the real (χ') and imaginary (χ'') components of the ac susceptibility at 2 K, for a polycrystalline sample of **2**.

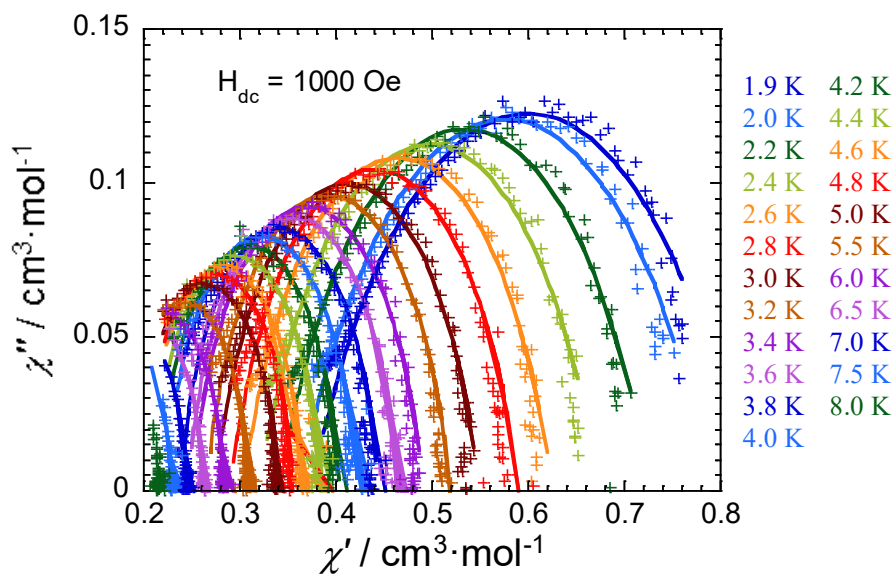


Figure S24. Experimental Cole-Cole Plots with generalized Debye fit of **2** at 1000 Oe DC field at different temperatures.

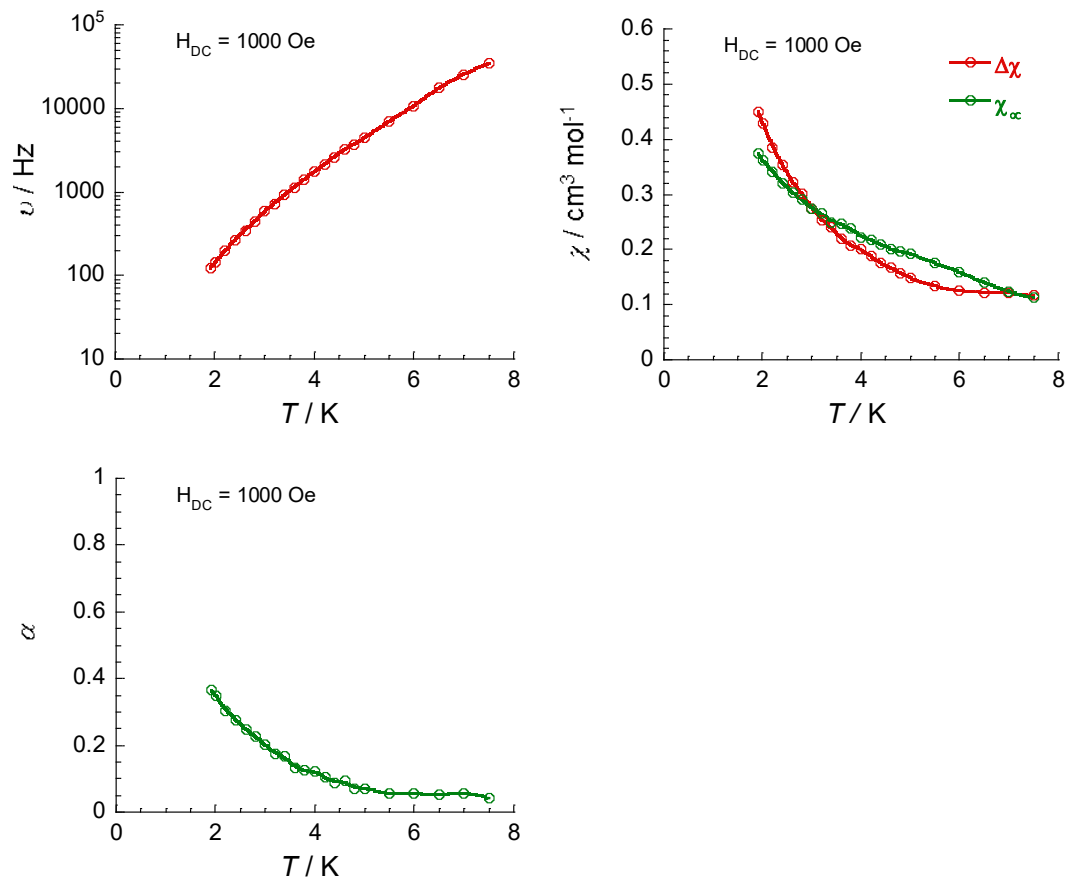


Figure S25. Temperature dependence of the parameters, α , ν , χ_0 and χ_∞ between 1.9 and 8 K deduced from the generalized Debye fit of the frequency dependence of the real (χ') and imaginary (χ'') components of the ac susceptibility at 1000 Oe, for a polycrystalline sample of **2**.

Table S4. Cole-Cole parameters for complex **2** at 1000 Oe

T (K)	α	χ_0	$\Delta\chi$
1.9100	0.36491	0.37395	0.45004
2.0100	0.34865	0.36134	0.42952
2.2100	0.30272	0.34116	0.38508
2.4100	0.27702	0.32050	0.35261
2.6100	0.24666	0.30309	0.32209
2.8100	0.22704	0.28985	0.30050
3.0000	0.20084	0.27422	0.27485
3.2000	0.17471	0.26496	0.25408
3.4000	0.16717	0.24992	0.24072
3.6000	0.13123	0.24606	0.21934
3.8000	0.12442	0.23813	0.20685
4.0000	0.12279	0.22250	0.20074
4.2000	0.10383	0.21667	0.18756
4.4000	0.086969	0.21000	0.17479
4.6000	0.093278	0.20000	0.16656
4.8000	0.070776	0.19729	0.15741
5.0000	0.070000	0.19180	0.14860
5.5000	0.055582	0.17559	0.13387
6.0000	0.054880	0.15900	0.12500
6.5000	0.052541	0.14000	0.12200
7.0000	0.056638	0.12400	0.12100
7.5000	0.040984	0.11200	0.11700

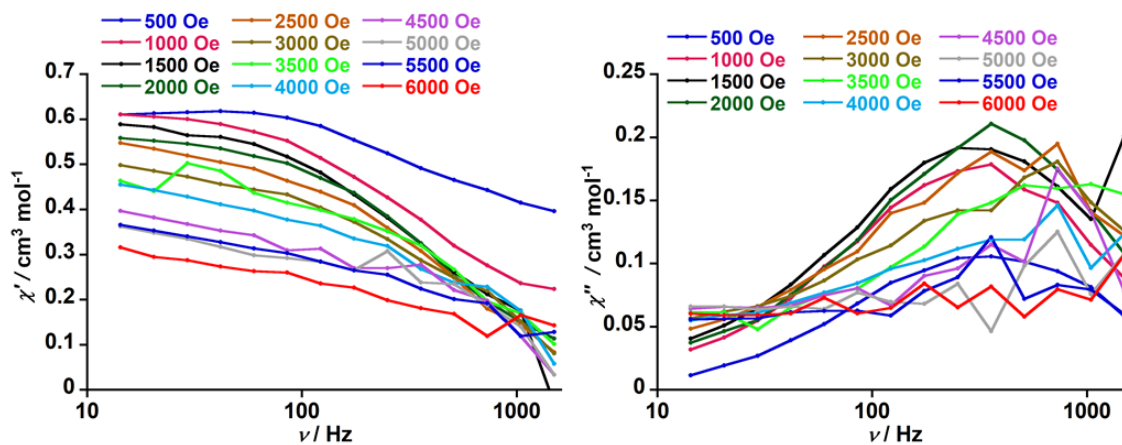


Figure S26. Frequency dependence of the real (χ' , left) and imaginary (χ'' , right) components of the ac susceptibility at different ac frequencies from 1 - 1500 Hz and different external dc field from 500 – 6000 Oe, respectively with a 3 Oe ac field for a polycrystalline sample of **3** at 1.8 K.

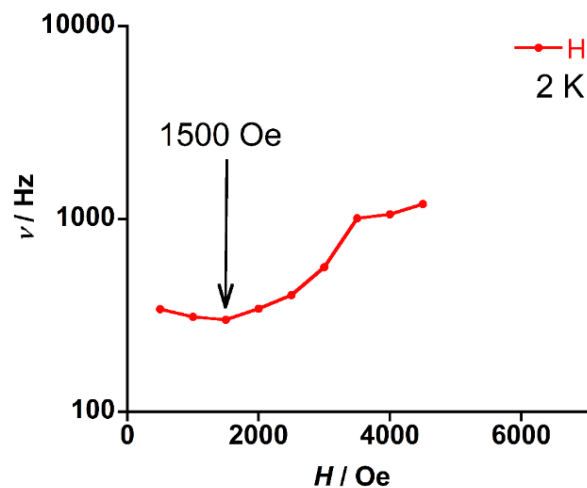


Figure S27. Field dependence of the characteristic relaxation frequency for **3** at 2 K.

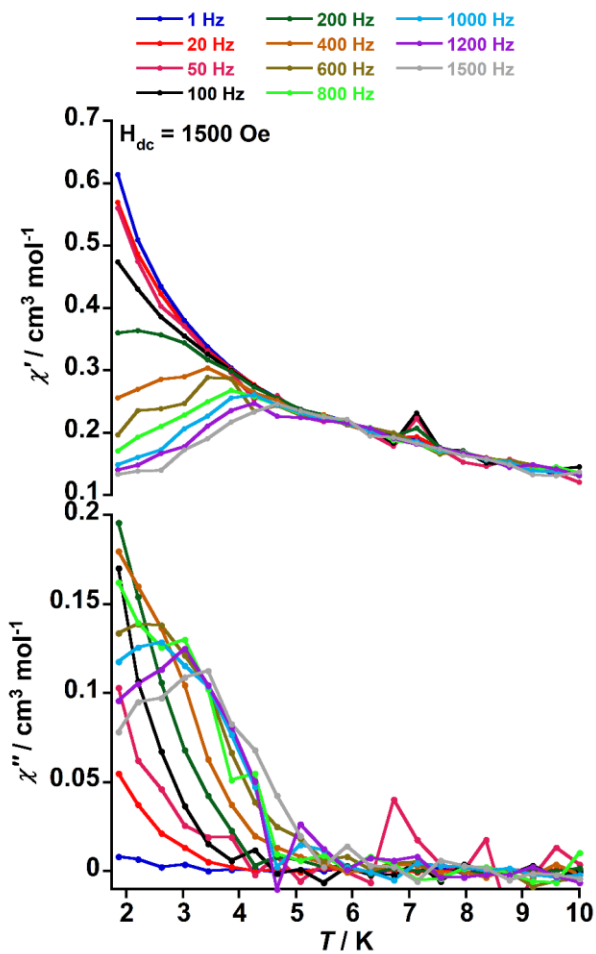


Figure S28. Frequency dependence of the real (χ' , top) and imaginary (χ'' , bottom) components of the ac susceptibility at different temperatures from 1.8 - 10 K and different ac frequencies from 1 - 1500 Hz, respectively, with a 3 Oe ac field for a polycrystalline sample of **3** at 1500 Oe external dc field.

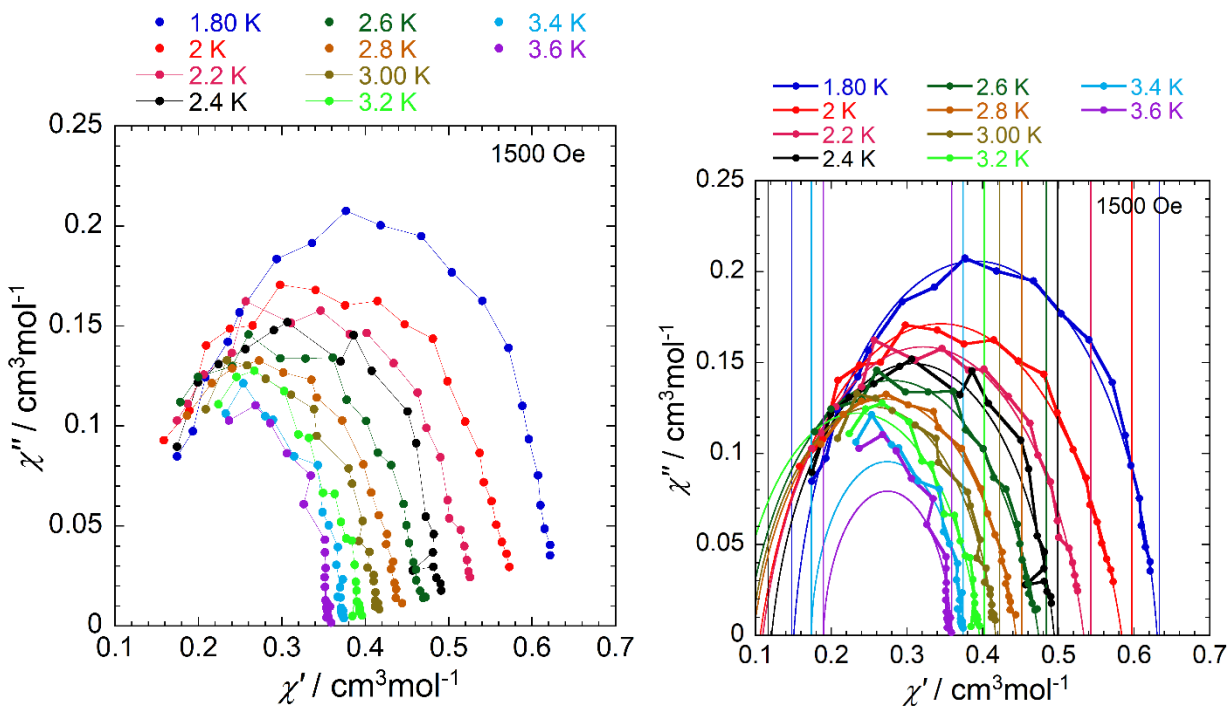


Figure S29. Experimental Cole-Cole Plots without fit (left) and with generalized Debye fit (right) of **3** at 1500 Oe DC field at different temperatures.

Table S5. Cole-Cole parameters for complex **3** at 1500 Oe

T (K)	α	χ_0	χ_{inf}
1.8000	0.097545	0.63057	0.15051
2.0000	0.20764	0.58387	0.10618
2.2000	0.18207	0.53367	0.10961
2.4000	0.14011	0.49451	0.12133
2.6000	0.20199	0.47401	0.086865
2.8000	0.18142	0.44414	0.097014
3.0000	0.15824	0.41738	0.094546
3.2000	0.17429	0.39581	0.073339
3.4000	0.030842	0.37425	0.1737
3.6000	0.04108	0.35886	0.18973

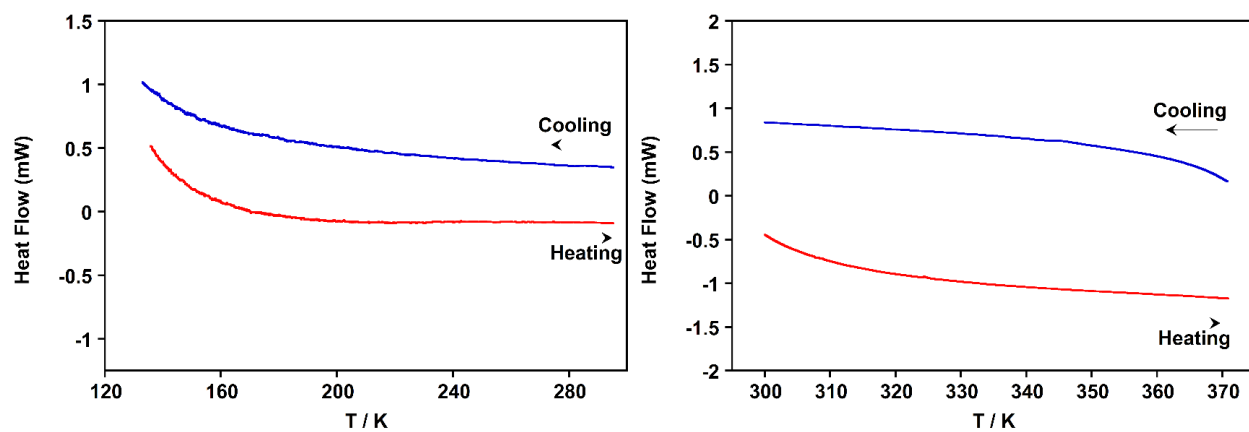


Figure S30. DSC plot of **1** from 295 – 130 K (left) and 295 – 372 K (right) at cooling/heating rates of 5 K/min. The heating and cooling modes are in red and blue lines, respectively.

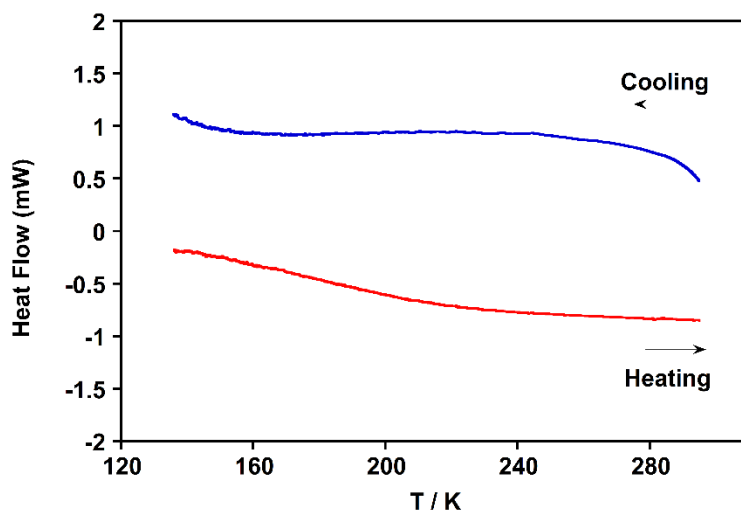


Figure S31. DSC plot of **2** from 295 – 130 K at cooling/heating rates of 5 K/min. The heating and cooling modes are in red and blue lines, respectively.

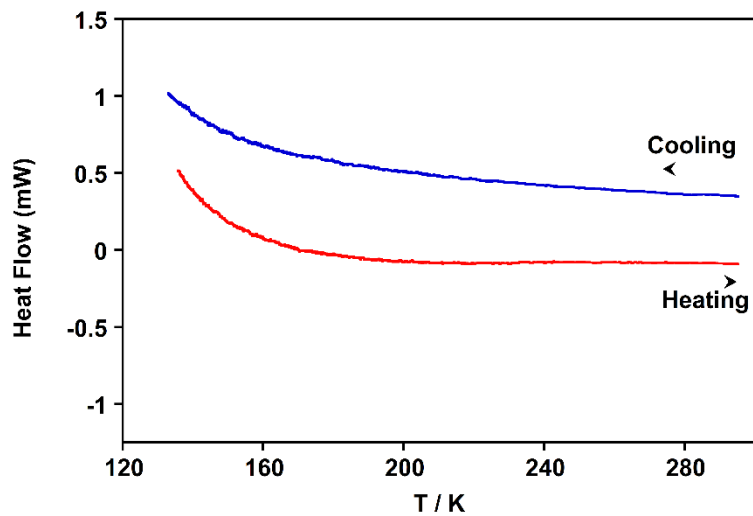


Figure S32. DSC plot of **3** from 295 – 130 K at cooling/heating rates of 5 K/ min. The heating and cooling modes are in red and blue lines, respectively.

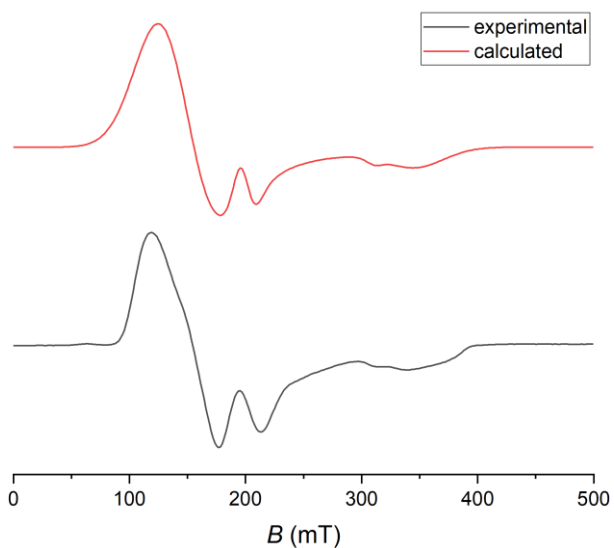


Figure S33. The X-band EPR data for **1** at $T = 5$ K. The calculated data corresponds to two Kramers doublets with $S_{\text{eff}} = 1/2$, first doublet with $g_{xy} = 4.781$, $g_z = 1.927$, linewidth = 58.5 mT; second doublet with $g_{xy} = 3.359$, $g_z = 2.148$, linewidth = 16.3 mT, where weight ratio between these two doublets are 1: 0.0496, respectively.

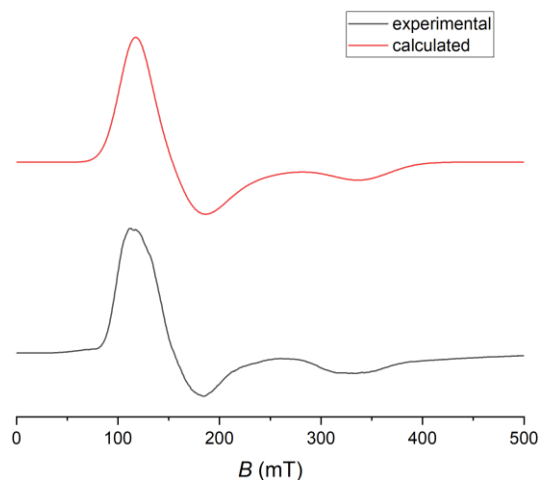


Figure S34. The X-band EPR data for **3** at $T = 5$ K. The calculated data corresponds to Kramers doublet with $S_{\text{eff}} = 1/2$ using $g_x = 5.669$, $g_y = 4.169$, $g_z = 1.954$, and H-strain defined as (2742, 3360, 1801) MHz.

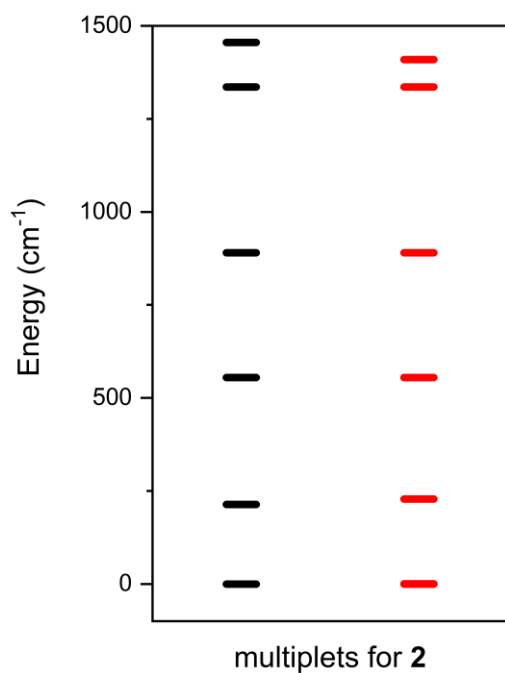


Figure S35. The multiplet energy levels calculated by CASSCF/NEVPT2 for [Co(bbp)(NCS)₂(DMF)] complex of **2** (black) and reconstructed energy levels with Figgis-Griffith Hamiltonian (eq.5) (red) using following parameters: $\alpha \cdot \lambda = -245 \text{ cm}^{-1}$, $\Delta_{\text{ax}} = -714 \text{ cm}^{-1}$, $\Delta_{\text{th}} = -151 \text{ cm}^{-1}$.

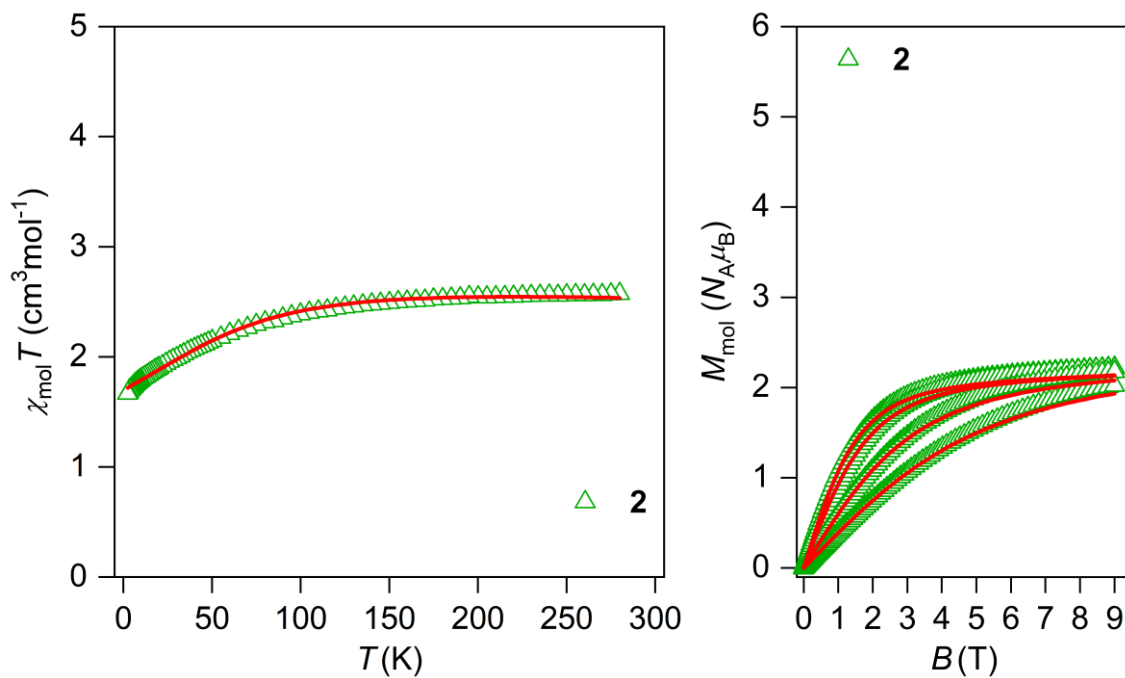


Figure S36. The magnetic data for **2**. The empty symbols – experimental data, full lines – calculated data using L-S Hamiltonian with parameters in text.

Table S6. Magnetic anisotropy and SMM parameters for mononuclear Co(II) hexa-, penta- and tetra coordinated complexes

Hexa-coordinated						
Complex	D (cm ⁻¹)	E (cm ⁻¹)	Magnetic behavior	τ_0 (s)	U_{eff} (cm ⁻¹)	Ref.
[Co(pydm) ₂](dnbz) ₂	44	24	SMM	2.8×10^{-9}	30.7051	1
[Co(PzOx) ₃ (BC ₆ H ₅)]Cl	-82	-0.246	SMM @ zero Oe dc	2.07×10^{-9}	152	2
			SMM @ 1500 Oe dc	1.25×10^{-9}	152	
[Co(abpt) ₂ (H ₂ O) ₂](N{C(CN) ₂ }) ₂ ·H ₂ O	34.9	11.412	SMM	1.04×10^{-7}	30.64	3
[Co(abpt) ₂ (H ₂ O) ₂](NO ₂ {C(CN) ₂ }) ₂	31.0	10.323	SMM	2.96×10^{-5}	8.549	3
[Co(abpt) ₂ (CH ₃ OH) ₂](C(CN){C(CN) ₂ }) ₂	37.8	11.642	SMM	-	-	3
[Co(abpt) ₂ (NO ₂ NCN) ₂]	41.4	9.439	SMM	2.19×10^{-5}	8.34	3
[Co(abpt) ₂ (NCSe) ₂]	37.7	5.089	SMM	7.76×10^{-6}	11.8	3
[Co(abpt) ₂ (ONC(CN) ₂) ₂]	-	-	SMM	1.63×10^{-6}	19.808	3
[Co(H ₂ L1) ₂].2THF	-30.4	6.9	SMM @ 1000 Oe dc	8.35×10^{-6}	5.074	4
[Co(HL2) ₂]	-18.4	4.3	SMM @ 1000 Oe dc	6.13×10^{-6}	7.075	4
[Co(H ₂ L3) ₂].CH ₂ Cl ₂	-27.4	5.0	SMM @ 1000 Oe dc	1.16×10^{-5}	9.799	4
[Co(bim) ₄ (tcm) ₂]	46.1	0.184	SMM	-	11.0	5
[Co(bmim) ₄ (tcm) ₂]	80.1	1.522	SMM	9.2×10^{-7}	9.0	5
[Co(hfa) ₂ (pic) ₂]	24.17	6.90	SMM	7.04×10^{-7}	17.167	6
(Tp) ₂ Co-1	-	-	SMM @ 800 Oe dc	3.07×10^{-8}	41.9	7
			SMM @ 3000 Oe dc	8.76×10^{-8}	35.79	
(Tp) ₂ Co-2	-	-	SMM @ 800 Oe dc	9.36×10^{-6}	10.42	7
			SMM @ 3000 Oe dc	3.66×10^{-7}	29.88	
Tp ₂ Co-2[(CH ₃) ₂ NCS ₂] ₃ Co	-	-	SMM @ 800 Oe dc	1.32×10^{-6}	22.65	7

			SMM @ 3000 Oe dc	1.82×10^{-8}	44.06	
(pzTp ^{Me}) ₂ Co	-	-	SMM @ 800 Oe dc	4.08×10^{-7}	20.15	7
			SMM @ 3000 Oe dc	1.40×10^{-6}	15.56	
[Co(2,6-dfba) ₂ (bpp) ₂ (H ₂ O) ₂] _n	53.19	7.68	SMM	5.9×10^{-7}	19.808	8
[Co(2,6-dfba) ₂ (bpe) ₂ (H ₂ O) ₂] _n	65.67	4.47	SMM	2.02×10^{-6}	15.43	8
[Co(abpt) ₂ (N ₃) ₂]	-24.1	-7.471	SMM	7.7×10^{-7}	20.155	9
[Co(imidazole) ₆][BPh ₄] ₂ ·0.3CH ₃ CN	-71.51	13.03	SMM	1.5×10^{-6}	15.013	10
[Co(imidazole) ₆][NO ₃] ₂	-41.2	4.22	SMM	4.5×10^{-6}	4.379	10
[Co ^{II} (Tpm)] ₂ [ClO ₄] ₂	-92	10.5	SMM	2.2-3.3 ($\times 10^{-7}$)	30.6-33.6	11
[Co ^{III} (Tpm)] ₂ [BPh ₄] ₂ ·2MeCN	-93	11.5	SMM	1.0-1.5 ($\times 10^{-7}$)	42.5-44.7	11
[Co(AcPyOx) ₃ BC ₆ H ₅] ₂ ClO ₄	-78	-	SMM @ zero Oe dc	2.07×10^{-9}	44.5	12
			SMM @ 1000 Oe dc	1.25×10^{-9}	70.5	
[Co(neo)(PhCOO) ₂](C ₂ /c) (α)	-1362	-160	SMM	6.51×10^{-7}	15.35	13
[Co(neo)(PhCOO) ₂](P ₂ ₁ /c) (β)	58.7	0	SMM	8.52×10^{-7}	11.884	13
[Co(3,5-dnb) ₂ (py) ₂ (H ₂ O) ₂](C ₂ /c)	58	0.1	SMM	1.37×10^{-7}	19.5	14
[Co(3,5-dnb) ₂ (py) ₂ (H ₂ O) ₂](P ₂ ₁ /c)	92	0.1	SMM	3.4×10^{-8}	21.1	14
[Co(L ¹) ₂](ClO ₄) ₂	61.1	-5.5	SMM	7.18×10^{-7}	10.286	15
[Co(L ²) ₂](ClO ₄) ₂	68.1	-5.7	SMM	2.06×10^{-8}	18.974	15
[Co(L ²) ₂](ClO ₄) ₂ ·MeCN	56.4	-10.5	SMM	3.44×10^{-7}	15.708	15
[Co(L ³) ₂](ClO ₄) ₂	-66.4	10.2	SMM	2.07×10^{-7}	21.407	15
[Co(L ⁴) ₂](ClO ₄) ₂	62.9	-2.4	SMM	4.95×10^{-7}	14.179	15
[Co(L ⁵) ₂](ClO ₄) ₂	74.9	-2.7	SMM	1.67×10^{-6}	5.6	15

Penta-coordinated						
Complex	D (cm ⁻¹)	E (cm ⁻¹)	Magnetic behavior	τ_0 (s)	U_{eff} (cm ⁻¹)	Ref.
[Co(bpdmpz)Cl]ClO ₄	4.9	1.274	SMM	-	10.186	16
[Co(bpdmpz)Cl]PF ₆	5.7	1.197	SMM @1000 Oe dc	-	11.764	16
[Co(bdmpzp)Cl]ClO ₄ ·H ₂ O	-4.6	-1.012	SMM	-	-8.391	16
[Co(bdmpzp)Cl]PF ₆	-4.4	-1.144	-	-	-8.391	16
[Co(tdmpza)Cl]ClO ₄	-5.2	0	-	-	-9.560	16
[CoCl ₂ L ^{C0}] ₂	61.9	0	SMM	1.69 × 10 ⁻⁷	31.3	17
[CoCl ₂ L ^{C7}] ₂	153	14.9	SMM	1.07 × 10 ⁻⁷	14.6	17
CoCl ₂ L ^{C10} ∞	70.1	8.9	-	-	-	17
[CoCl ₂ L ^{C12}] _∞	46.8	0.9	SMM	5.96 × 10 ⁻⁸	40.5	17
[CoCl ₂ L ^{C14}] ₂	87.5	0	-	-	-	17
[Co(L3A)Cl ₂]	45.7	10.968	SMM	-	-	18
[Co(L3B)Cl ₂]	38.4	11.904	SMM	-	-	18
[Co(L3C)Cl ₂]·CH ₂ Cl ₂	-43.9	-11.414	SMM	-	-	18
[Co(L3D)Cl ₂]	-41.3	0	SMM	5.28 × 10 ⁻⁹	15.846	18
[Co(Me ₆ tren)Cl](ClO ₄)	4.9	-	SMM	3.6 × 10 ⁻⁹	14.039	19
[Co(bbp)Cl ₂]·(MeOH)	14.5	0	SMM	5.8 × 10 ⁻⁵	13.622	20
[Co(bbp)Br ₂]·(MeOH)	8.4	0	SMM	3.1 × 10 ⁻⁵	5.699	20
[Co(bbp)(NCS) ₂]	10.7	1.1 × 10 ⁻⁴	SMM	4.6 × 10 ⁻⁵	6.742	20
[Co(12-TMC)(CH ₃ CN)](BF ₄) ₂	-	-	SMM @ 2500 Oe dc	-	-	21
[Co(12-TMC)(CH ₃ CN)](PF ₆) ₂	-	-	SMM @ 2500 Oe dc	-	-	21
[Co ^{II} (Me ₆ tren)(OH ₂)](NO ₃) ₂	-	-	SMM	9.6 × 10 ⁻⁹	12.5	22
[Co(NS ₃ ^{iPr})Cl](BPh ₄)	-19.9	1.5	SMM	-	-	23
([ArN=CMe] ₂ (NPh))Co(NCS) ₂	-28.147	-	SMM	3.6 × 10 ⁻⁶	11.12	24
([ArN=CPh] ₂ (NPh))Co(NCS) ₂	-28.217	-	SMM	5.1 × 10 ⁻⁷	16.68	24
[Co(phen)(DMSO)Cl ₂]	-17	-4.08	SMM	5.69 × 10 ⁻⁹	7.228	15

Tetra-coordinated						
Complex	D (cm ⁻¹)	E (cm ⁻¹)	Magnetic behavior	τ_0 (s)	U_{eff} (cm ⁻¹)	Ref.
[Co(1,2- dithiol-o-carborane)]	-71.6	0.27	SMM	3.3×10^{-6}	26.8	16
[Co ^{II} (dmbpy) ₂](ClO ₄) ₂	-50.6	-	SMM	-	-	17
[Co ^{II} (dmbpy) ₂ (H ₂ O)](ClO ₄) ₂	35.8	-	SMM	-	-	17
[Co(xantpo)(NCS) ₂]	-7.11	2.23	SMM	-	-	18
[Co(xantpo)(NCO) ₂]	12.6	0.8	SMM	-	-	18
[Co(bmim) ₂ (SCN) ₂]	-7.5	-0.795	SMM @ 500 Oe dc	2.15×10^{-9}	15.3	19
			SMM @ 1000 Oe dc	2.08×10^{-9}	15.6	
			SMM @ 2500 Oe dc	3.61×10^{-9}	14.7	
[Co(bmim) ₂ (NCO) ₂]	6.3	0.044	SMM @ 1000 Oe dc	6.8×10^{-9}	10.8	19
			SMM @ 2500 Oe dc	1.7×10^{-8}	9.7	
[Co(bmim) ₂ (N ₃) ₂]	6.7	0.603	SMM @ 1000 Oe dc	2.5×10^{-8}	6.67	19
			SMM @ 2500 Oe dc	3.2×10^{-8}	7.51	
[K(C ₁₂ H ₂₄ O ₆) ₂][Co(NCS) ₄]	2.67	0.01	SMM	-	-	20
[Ba(C ₁₂ H ₂₄ O ₆) ₃ ·3H ₂ O][Co(NCS) ₄]	5.20	0.02	SMM	-	-	20
[Co(Cyt) ₂ (NCS) ₂]	-6.1	-0.762	SMM	3.41×10^{-8}	13.0	21
[Co(Cyt) ₂ (NCO) ₂]	-7.4	-1.258	SMM	4.17×10^{-8}	19.1	21
[Co(L ₁) ₄](NO ₃) ₂	-61.7	-3.085	SMM	2.24×10^{-6}	32.0	22
[Co(L ₂) ₄](ClO ₄) ₂	-80.7	-1.614	SMM	2.49×10^{-6}	32.7	22
[Co(bcp)Cl ₂]	-5.62	-	SMM	1.27×10^{-11}	33.222	23
(HNEt ₃) ₂ [Co(pdms) ₂]	-115	-	SMM	3.89×10^{-8}	118	24
[Co(PPh ₃) ₂ (NCS) ₂]	-9.4	-	SMM	-	-	25
[Co(biq)Cl ₂]	10.5	0	SMM	1.9×10^{-10}	29.608	26
[Co(biq)Br ₂]	12.5	0	SMM	1.2×10^{-10}	27.523	26
[Co(biq)I ₂]	10.3	4.1	SMM	3.2×10^{-13}	39.615	26
[Co ^{II} (bzi) ₂ (NCS) ₂]	-10.1	-	SMM	1.86×10^{-8}	14.7	27
Co(BrL) ₂ ·3CH ₃ OH	-44.0	<0.01	SMM	2.2×10^{-6}	12.823	28
Co(PL) ₂ ·2CH ₃ OH	-50.0	<0.01	SMM	1.6×10^{-9}	35.03	28

Appendix

Complex 1:

checkCIF/PLATON report

Structure factors have been supplied for datablock(s) 1

THIS REPORT IS FOR GUIDANCE ONLY. IF USED AS PART OF A REVIEW PROCEDURE FOR PUBLICATION, IT SHOULD NOT REPLACE THE EXPERTISE OF AN EXPERIENCED CRYSTALLOGRAPHIC REFEREE.

No syntax errors found. CIF dictionary Interpreting this report

Datablock: 1

Bond precision: C-C = 0.0054 Å

Wavelength=0.71073

Cell: a=10.4390(4) b=17.1419(6) c=17.3692(6)
 alpha=90.118(2) beta=103.278(2) gamma=93.755(2) Temperature: 120 K

	Calculated	Reported
Volume	3018.07(19)	3018.07(19)
Space group	P -1	P -1
Hall group	-P 1	-P 1
C38 H26 Co N10, C4 Co N4		
Moiety formula		?
S4, 4(C3 H7 N O)		
Sum formula	C54 H54 Co2 N18 O4 S4	C54 H54 Co2 N18 O4 S4
Mr	1265.25	1265.25
Dx,g cm-3	1.392	1.392
Z	2	2
Mu (mm-1)	0.748	0.748
F000	1308.0	1308.0
F000'	1310.73	
h,k,lmax	12,20,20	12,20,20

Nref	11127	11102
Tmin,Tmax	0.764,0.829	0.848,0.943
Tmin'	0.741	

Correction method= # Reported T Limits: Tmin=0.848 Tmax=0.943


AbsCorr = MULTI-SCAN

Data completeness= 0.998 Theta(max)= 25.399

R(reflections)= 0.0600(8950) wR2(reflections)= 0.1576(11102)

S = 1.046 Npar= 757

The following ALERTS were generated. Each ALERT has the format `test-name_ALERT_alert-type_alert-level`. Click on the hyperlinks for more details of the test.

-  **Alert level C**
- PLAT220_ALERT_2_C NonSolvent Resd 1 C Ueq(max) / Ueq(min) Range 3.8 Ratio
- PLAT241_ALERT_2_C High MainMol Ueq as Compared to Neighbors of C10 Check
- PLAT241_ALERT_2_C High MainMol Ueq as Compared to Neighbors of N11 Check
- PLAT242_ALERT_2_C Low MainMol Ueq as Compared to Neighbors of C41 Check
- PLAT244_ALERT_4_C Low Solvent Ueq as Compared to Neighbors of N17 Check
- PLAT244_ALERT_4_C Low Solvent Ueq as Compared to Neighbors of N18 Check
- PLAT250_ALERT_2_C Large U3/U1 Ratio for Average U(i,j) Tensor 4.0 Note
- PLAT260_ALERT_2_C Large Average Ueq of Residue Including O3A 0.134 Check
- PLAT413_ALERT_2_C Short Inter XH3 .. XHn H44B ..H51 . 2.11 Ang.
- 1+x,y,-1+z = 1_454 Check
- PLAT906_ALERT_3_C Large K Value in the Analysis of Variance 2.471 Check
- PLAT911_ALERT_3_C Missing FCF Refl Between Thmin & STh/L= 0.600 8 Report
- PLAT977_ALERT_2_C Check Negative Difference Density on H44A -0.41 eA-3
- PLAT977_ALERT_2_C Check Negative Difference Density on H44C -0.42 eA-3
- PLAT977_ALERT_2_C Check Negative Difference Density on H45A -0.48 eA-3
- PLAT977_ALERT_2_C Check Negative Difference Density on H45B -0.40 eA-3

PLAT977_ALERT_2_C Check Negative Difference Density on H47A	-0.31 eA-3
PLAT977_ALERT_2_C Check Negative Difference Density on H48A	-0.32 eA-3
PLAT977_ALERT_2_C Check Negative Difference Density on H48B	-0.36 eA-3
PLAT977_ALERT_2_C Check Negative Difference Density on H48C	-0.32 eA-3
PLAT977_ALERT_2_C Check Negative Difference Density on H52A	-0.38 eA-3
PLAT977_ALERT_2_C Check Negative Difference Density on H52B	-0.34 eA-3
PLAT977_ALERT_2_C Check Negative Difference Density on H52C	-0.36 eA-3
PLAT978_ALERT_2_C Number C-C Bonds with Positive Residual Density.	0 Info

Alert level G

PLAT002_ALERT_2_G Number of Distance or Angle Restraints on AtSite	10 Note
PLAT003_ALERT_2_G Number of Uiso or Uij Restrained non-H Atoms ...	6 Report
PLAT007_ALERT_5_G Number of Unrefined Donor-H Atoms	4 Report
PLAT083_ALERT_2_G SHELXL Second Parameter in WGHT Unusually Large	9.56 Why ?
PLAT154_ALERT_1_G The s.u.'s on the Cell Angles are Equal ..(Note)	0.002 Degree
PLAT171_ALERT_4_G The CIF-Embedded .res File Contains EADP Records	3 Report
PLAT176_ALERT_4_G The CIF-Embedded .res File Contains SADI Records	3 Report
PLAT178_ALERT_4_G The CIF-Embedded .res File Contains SIMU Records	2 Report
PLAT300_ALERT_4_G Atom Site Occupancy of S2B Constrained at	0.5 Check
PLAT300_ALERT_4_G Atom Site Occupancy of S2A Constrained at	0.3 Check
PLAT300_ALERT_4_G Atom Site Occupancy of S2C Constrained at	0.2 Check
PLAT300_ALERT_4_G Atom Site Occupancy of N12B Constrained at	0.5 Check
PLAT300_ALERT_4_G Atom Site Occupancy of C40B Constrained at	0.5 Check
PLAT300_ALERT_4_G Atom Site Occupancy of N12A Constrained at	0.3 Check
PLAT300_ALERT_4_G Atom Site Occupancy of N12C Constrained at	0.2 Check
PLAT300_ALERT_4_G Atom Site Occupancy of C40A Constrained at	0.3 Check
PLAT300_ALERT_4_G Atom Site Occupancy of C40C Constrained at	0.2 Check
PLAT302_ALERT_4_G Anion/Solvent/Minor-Residue Disorder (Resd 2)	23% Note
PLAT380_ALERT_4_G Incorrectly? Oriented X(sp2)-Methyl Moiety	C44 Check
PLAT380_ALERT_4_G Incorrectly? Oriented X(sp2)-Methyl Moiety	C45 Check

PLAT380_ALERT_4_G Incorrectly? Oriented X(sp ²)-Methyl Moiety	C47 Check
PLAT380_ALERT_4_G Incorrectly? Oriented X(sp ²)-Methyl Moiety	C48 Check
PLAT380_ALERT_4_G Incorrectly? Oriented X(sp ²)-Methyl Moiety	C50A Check
PLAT380_ALERT_4_G Incorrectly? Oriented X(sp ²)-Methyl Moiety	C55A Check
PLAT380_ALERT_4_G Incorrectly? Oriented X(sp ²)-Methyl Moiety	C52 Check
PLAT380_ALERT_4_G Incorrectly? Oriented X(sp ²)-Methyl Moiety	C53 Check
PLAT790_ALERT_4_G Centre of Gravity not Within Unit Cell: Resd. #	3 Note
C3 H7 N O	PLAT790_ALERT_4_G Centre of Gravity not Within
Unit Cell: Resd. #	4 Note
C3 H7 N O	
PLAT794_ALERT_5_G Tentative Bond Valency for Co1 (II) .	1.94 Info
PLAT860_ALERT_3_G Number of Least-Squares Restraints	45 Note
No Info/Value for _atom_sites_solution_primary .	Please Do !
PLAT910_ALERT_3_G Missing # of FCF Reflection(s) Below Theta(Min).	2 Note
PLAT912_ALERT_4_G Missing # of FCF Reflections Above STh/L= 0.600	15 Note

0 ALERT level A = Most likely a serious problem - resolve or explain

0 ALERT level B = A potentially serious problem, consider carefully

23 ALERT level C = Check. Ensure it is not caused by an omission or oversight

33 ALERT level G = General information/check it is not something unexpected

2 ALERT type 1 CIF construction/syntax error, inconsistent or missing data

22 ALERT type 2 Indicator that the structure model may be wrong or deficient

4 ALERT type 3 Indicator that the structure quality may be low

26 ALERT type 4 Improvement, methodology, query or suggestion

2 ALERT type 5 Informative message, check

It is advisable to attempt to resolve as many as possible of the alerts in all categories. Often the minor alerts point to easily fixed oversights, errors and omissions in your CIF or refinement strategy, so attention to these fine details can be worthwhile. In order to resolve some of the more serious problems it may be necessary to carry out additional measurements or structure refinements. However, the purpose of your study may justify the reported deviations and the more serious of these

should normally be commented upon in the discussion or experimental section of a paper or in the "special_details" fields of the CIF. checkCIF was carefully designed to identify outliers and unusual parameters, but every test has its limitations and alerts that are not important in a particular case may appear. Conversely, the absence of alerts does not guarantee there are no aspects of the results needing attention. It is up to the individual to critically assess their own results and, if necessary, seek expert advice.

Publication of your CIF in IUCr journals

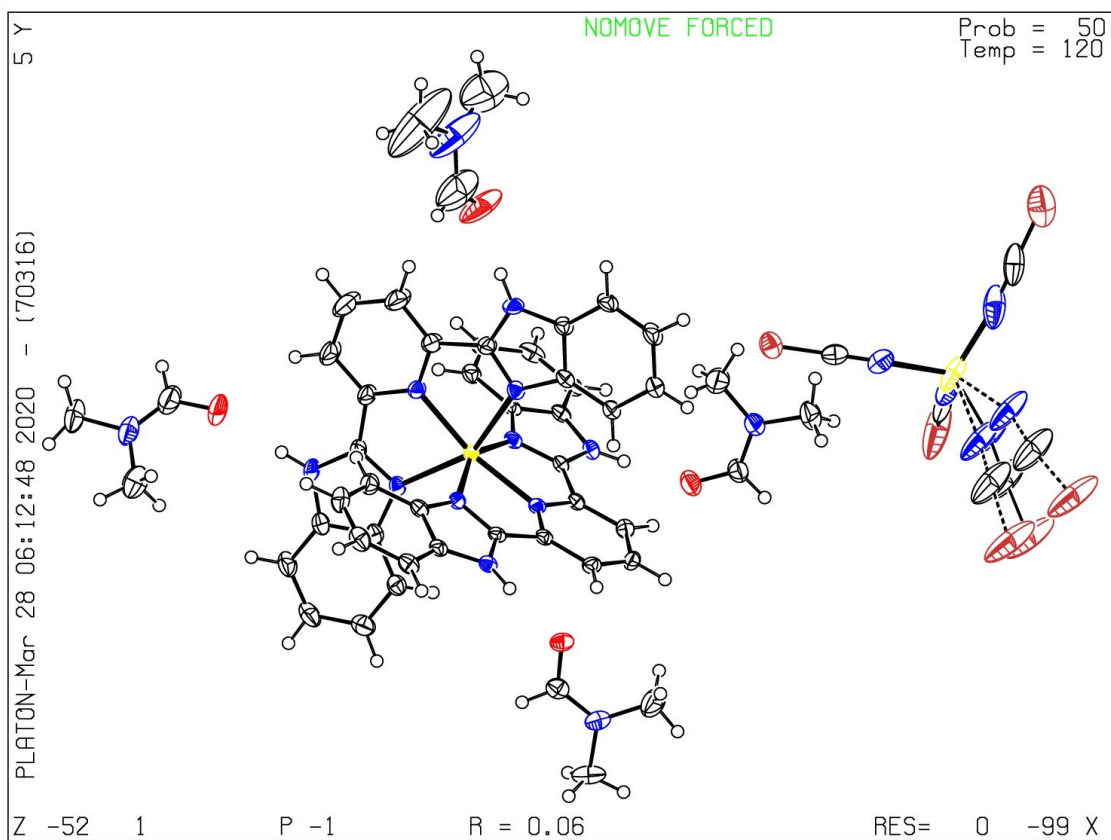
A basic structural check has been run on your CIF. These basic checks will be run on all CIFs submitted for publication in IUCr journals (*Acta Crystallographica*, *Journal of Applied Crystallography*, *Journal of Synchrotron Radiation*); however, if you intend to submit to *Acta Crystallographica Section C* or *E* or *IUCrData*, you should make sure that full publication checks are run on the final version of your CIF prior to submission.

Publication of your CIF in other journals

Please refer to the *Notes for Authors* of the relevant journal for any special instructions relating to CIF submission.

PLATON version of 22/12/2019; check.def file version of 13/12/2019

Datablock 1 - ellipsoid plot



Complex 2:

checkCIF/PLATON report

Structure factors have been supplied for datablock(s) 2

THIS REPORT IS FOR GUIDANCE ONLY. IF USED AS PART OF A REVIEW PROCEDURE FOR PUBLICATION, IT SHOULD NOT REPLACE THE EXPERTISE OF AN EXPERIENCED CRYSTALLOGRAPHIC REFEREE.

No syntax errors found. CIF dictionary Interpreting this report

Datablock: 2

Bond precision: C-C = 0.0059 Å

Wavelength=0.71073

Cell: a=11.6648(17) b=11.8019(17) c=12.8244(18) alpha=95.193(7)
beta=98.785(7) gamma=92.871(7) Temperature: 293 K

	Calculated	Reported
Volume	1734.0(4)	1734.0(4)
Space group	P -1	P -1
Hall group	-P 1	-P 1
C24 H20 Co N8 O S2, 2(C3		
Moiety formula		?
H7 N O)		
Sum formula	C30 H34 Co N10 O3 S2	C30 H34 Co N10 O3 S2
Mr	705.72	705.72
Dx, g cm ⁻³	1.352	1.352
Z	2	2
Mu (mm ⁻¹)	0.661	0.661
F000	734.0	734.0
F000'	735.40	
<hr/>		
h, k, lmax	15, 15, 16	15, 15, 16
Nref	7957	7913
Tmin, Tmax	0.764, 0.809	0.848, 0.943

Tmin' 0.748


Correction method= # Reported T Limits: Tmin=0.848 Tmax=0.943
AbsCorr = MULTI-SCAN

Data completeness= 0.994 Theta(max)= 27.484

R(reflections)= 0.0620(4550) wR2(reflections)= 0.1568(7913)


S = 1.000 Npar= 437

The following ALERTS were generated. Each ALERT has the format
test-name_ALERT_alert-type_alert-level. Click on the hyperlinks
for more details of the test.


 **Alert level B**

PLAT910_ALERT_3_B Missing # of FCF Reflection(s) Below Theta(Min). 12 Note

Comment: The alert "Missing # of FCF Reflection(s) Below Theta(Min)" is due to the error in measurement. The theta min for complex 2 is 3.23 which is higher than the average theta min value originating from the data collection strategy. Due to this higher theta min value some reflections are missing below this limit.

 **Alert level C**

PLAT230_ALERT_2_C Hirshfeld Test Diff for O1 --C22 . 5.7 s.u.
PLAT242_ALERT_2_C Low MainMol Ueq as Compared to Neighbors of N8 Check
PLAT242_ALERT_2_C Low MainMol Ueq as Compared to Neighbors of C20 Check
PLAT242_ALERT_2_C Low MainMol Ueq as Compared to Neighbors of C21 Check
PLAT244_ALERT_4_C Low Solvent Ueq as Compared to Neighbors of N10 Check
PLAT244_ALERT_4_C Low Solvent Ueq as Compared to Neighbors of N9 Check
PLAT351_ALERT_3_C Long C-H (X0.96,N1.08A) C30 - H30 . 1.12 Ang.
PLAT906_ALERT_3_C Large K Value in the Analysis of Variance 7.442 Check
PLAT906_ALERT_3_C Large K Value in the Analysis of Variance 2.207 Check

 **Alert level G**

PLAT154_ALERT_1_G The s.u.'s on the Cell Angles are Equal ..(Note) 0.007 Degree
PLAT164_ALERT_4_G Nr. of Refined C-H H-Atoms in Heavy-Atom Struct. 2 Note
PLAT199_ALERT_1_G Reported _cell_measurement_temperature (K) 293 Check
PLAT200_ALERT_1_G Reported _diffrn_ambient_temperature (K) 293 Check
PLAT230_ALERT_2_G Hirshfeld Test Diff for S2 --C21 . 5.5 s.u.
PLAT794_ALERT_5_G Tentative Bond Valency for Co1 (II) . 1.97 Info
PLAT883_ALERT_1_G No Info/Value for _atom_sites_solution_primary . Please Do !
PLAT912_ALERT_4_G Missing # of FCF Reflections Above STh/L= 0.600 33 Note
PLAT978_ALERT_2_G Number C-C Bonds with Positive Residual Density. 1 Info
PLAT992_ALERT_5_G Repd & Actual _reflns_number_gt Values Differ by 1 Check

0 **ALERT level A** = Most likely a serious problem - resolve or explain
1 **ALERT level B** = A potentially serious problem, consider carefully
9 **ALERT level C** = Check. Ensure it is not caused by an omission or oversight
10 **ALERT level G** = General information/check it is not something unexpected

4 ALERT type 1 CIF construction/syntax error, inconsistent or missing data
6 ALERT type 2 Indicator that the structure model may be wrong or deficient
4 ALERT type 3 Indicator that the structure quality may be low
4 ALERT type 4 Improvement, methodology, query or suggestion
2 ALERT type 5 Informative message, check

It is advisable to attempt to resolve as many as possible of the alerts in all categories. Often the minor alerts point to easily fixed oversights, errors and omissions in your CIF or refinement strategy, so attention to these fine details can be worthwhile. In order to resolve some of the more serious problems it may be necessary to carry out additional measurements or structure refinements. However, the purpose of your study may justify the reported deviations and the more serious of these should normally be commented upon in the discussion or experimental section of a paper or in the "special_details" fields of the CIF. checkCIF was carefully designed to identify outliers and unusual parameters, but every test has its limitations and alerts that are not important in a particular case may appear. Conversely, the absence of alerts does not guarantee there are no aspects of the results needing attention. It is up to the individual to critically assess their own results and, if necessary, seek expert advice.

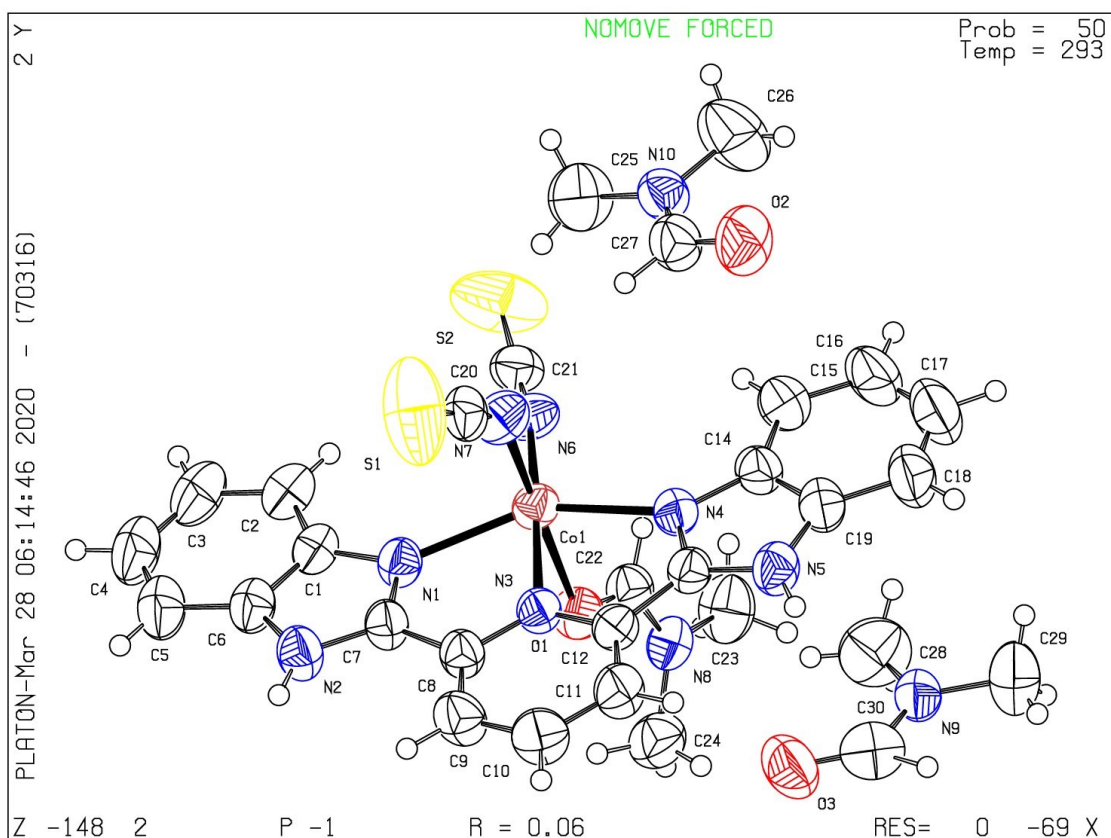
Publication of your CIF in IUCr journals

A basic structural check has been run on your CIF. These basic checks will be run on all CIFs submitted for publication in IUCr journals (*Acta Crystallographica*, *Journal of Applied Crystallography*, *Journal of Synchrotron Radiation*); however, if you intend to submit to *Acta Crystallographica Section C* or *E* or *IUCrData*, you should make sure that full publication checks are run on the final version of your CIF prior to submission.

Publication of your CIF in other journals

Please refer to the *Notes for Authors* of the relevant journal for any special instructions relating to CIF submission.

PLATON version of 22/12/2019; check.def file version of 13/12/2019

**Complex 3:****checkCIF/PLATON report**

Structure factors have been supplied for datablock(s) 3

THIS REPORT IS FOR GUIDANCE ONLY. IF USED AS PART OF A REVIEW PROCEDURE FOR PUBLICATION, IT SHOULD NOT REPLACE THE EXPERTISE OF AN EXPERIENCED CRYSTALLOGRAPHIC REFEREE.

No syntax errors found. CIF dictionary Interpreting this report

Datablock: 3

Bond precision: C-C = 0.0040 Å

Wavelength=0.71073

Cell: a=9.4850 (6)

 b=9.8536 (7)

 c=11.3697 (8)

 alpha=100.998 (3) beta=91.074 (3) gamma=106.602 (3)

Temperature: 120 K

	Calculated	Reported
Volume	996.59(12)	996.59(12)
Space group	P -1	P -1
Hall group	-P 1	-P 1
Moiety formula	C21 H13 Co N7 S2	?
Sum formula	C21 H13 Co N7 S2	C21 H13 Co N7 S2
Mr	486.43	486.45
Dx, g cm-3	1.621	1.621
Z	2	2
Mu (mm-1)	1.096	1.096
F000	494.0	494.0
F000'	495.29	
h, k, lmax	11, 11, 13	11, 11, 13
Nref	3668	3661
Tmin, Tmax	0.708, 0.839	0.848, 0.943
Tmin'	0.675	

Correction method= # Reported T Limits: Tmin=0.848 Tmax=0.943
AbsCorr = MULTI-SCAN

Data completeness= 0.998

Theta(max)= 25.398

R(reflections)= 0.0326(2977)

wR2(reflections)= 0.0740(3661)

S = 1.022

Npar= 280

The following ALERTS were generated. Each ALERT has the format
name_ALERT_alert-type_alert-level.
Click on the hyperlinks for more details of the test.

test-



Alert level C

PLAT911_ALERT_3_C Missing FCF Refl Between Thmin & STh/L= 0.600 2 Report



Alert level G

PLAT007_ALERT_5_G Number of Unrefined Donor-H Atoms 2 Report
 PLAT154_ALERT_1_G The s.u.'s on the Cell Angles are Equal ..(Note) 0.003 Degree
 PLAT230_ALERT_2_G Hirshfeld Test Diff for S1 --C21 . 7.6 s.u.
 PLAT230_ALERT_2_G Hirshfeld Test Diff for S2 --C20 . 6.1 s.u.

PLAT794_ALERT_5_G	Tentative Bond Valency for Col	(II)	.	2.00	Info
PLAT883_ALERT_1_G	No Info/Value for _atom_sites_solution_primary	.			Please Do !
PLAT912_ALERT_4_G	Missing # of FCF Reflections Above STh/L=	0.600			4 Note
PLAT933_ALERT_2_G	Number of OMIT Records in Embedded .res File ...				2 Note
PLAT978_ALERT_2_G	Number C-C Bonds with Positive Residual Density.				3 Info

0 **ALERT level A** = Most likely a serious problem - resolve or explain
0 **ALERT level B** = A potentially serious problem, consider carefully
1 **ALERT level C** = Check. Ensure it is not caused by an omission or oversight
9 **ALERT level G** = General information/check it is not something unexpected

2 ALERT type 1 CIF construction/syntax error, inconsistent or missing data
4 ALERT type 2 Indicator that the structure model may be wrong or deficient
1 ALERT type 3 Indicator that the structure quality may be low
1 ALERT type 4 Improvement, methodology, query or suggestion
2 ALERT type 5 Informative message, check

It is advisable to attempt to resolve as many as possible of the alerts in all categories. Often the minor alerts point to easily fixed oversights, errors and omissions in your CIF or refinement strategy, so attention to these fine details can be worthwhile. In order to resolve some of the more serious problems it may be necessary to carry out additional measurements or structure refinements. However, the purpose of your study may justify the reported deviations and the more serious of these should normally be commented upon in the discussion or experimental section of a paper or in the "special_details" fields of the CIF. checkCIF was carefully designed to identify outliers and unusual parameters, but every test has its limitations and alerts that are not important in a particular case may appear. Conversely, the absence of alerts does not guarantee there are no aspects of the results needing attention. It is up to the individual to critically assess their own results and, if necessary, seek expert advice.

Publication of your CIF in IUCr journals

A basic structural check has been run on your CIF. These basic checks will be run on all CIFs submitted for publication in IUCr journals (*Acta Crystallographica*, *Journal of Applied Crystallography*, *Journal of Synchrotron Radiation*); however, if you intend to submit to *Acta Crystallographica Section C* or *E* or *IUCrData*, you should make sure that full publication checks are run on the final version of your CIF prior to submission.

Publication of your CIF in other journals

Please refer to the *Notes for Authors* of the relevant journal for any special instructions relating to CIF submission.

PLATON version of 22/12/2019; check.def file version of 13/12/2019

Datablock 3 - ellipsoid plot

References:

- (1) Valigura, D.; Rajnák, C.; Moncol, J.; Titiš, J.; Boča, R. A Mononuclear Co(II) Complex Formed from Pyridinedimethanol with Manifold Slow Relaxation Channels. *Dalton Trans.* **2017**, *46*, 10950–10956.
- (2) Novikov, V. V.; Pavlov, A. A.; Nelyubina, Y. V.; Boulon, M.-E.; Varzatskii, O. A.; Voloshin, Y. Z.; Winpenny, R. E. P. A Trigonal Prismatic Mononuclear Cobalt(II) Complex Showing Single-Molecule Magnet Behavior. *J. Am. Chem. Soc.* **2015**, *137*, 9792–9795.
- (3) Váhovská, L.; Vitushkina, S.; Potočňák, I.; Trávníček, Z.; Herchel, R. Effect of Linear and Non-Linear Pseudohalides on the Structural and Magnetic Properties of Co(II) Hexacoordinate Single-Molecule Magnets. *Dalton Trans.* **2018**, *47*, 1498–1512.
- (4) Peng, Y.; Mereacre, V.; Anson, C. E.; Zhang, Y.; Bodenstein, T.; Fink, K.; Powell, A. K. Field-Induced Co(II) Single-Ion Magnets with Mer-Directing Ligands but Ambiguous Coordination Geometry. *Inorg. Chem.* **2017**, *56*, 6056–6066.
- (5) Świtlicka, A.; Palion-Gazda, J.; Machura, B.; Cano, J.; Lloret, F.; Julve, M. Field-Induced Slow Magnetic Relaxation in Pseudooctahedral Cobalt(II) Complexes with Positive Axial and Large Rhombic Anisotropy. *Dalton Trans.* **2019**, *48*, 1404–1417.
- (6) Novitchi, G.; Jiang, S.; Shova, S.; Rida, F.; Hlavička, I.; Orlita, M.; Wernsdorfer, W.; Hamze, R.; Martins, C.; Suaud, N.; et al. From Positive to Negative Zero-Field Splitting in a Series of Strongly Magnetically Anisotropic Mononuclear Metal Complexes. *Inorg. Chem.* **2017**, *56*, 14809–14822.
- (7) Zhang, J.; Li, J.; Yang, L.; Yuan, C.; Zhang, Y.-Q.; Song, Y. Magnetic Anisotropy from Trigonal Prismatic to Trigonal Antiprismatic Co(II) Complexes: Experimental Observation and Theoretical Prediction. *Inorg. Chem.* **2018**, *57*, 3903–3912.
- (8) Wu, Y.; Tian, D.; Ferrando-Soria, J.; Cano, J.; Yin, L.; Ouyang, Z.; Wang, Z.; Luo, S.; Liu, X.; Pardo, E. Modulation of the Magnetic Anisotropy of Octahedral Cobalt(II) Single-Ion Magnets by Fine-Tuning the Axial Coordination Microenvironment. *Inorg. Chem. Front.* **2019**, *6*, 848–856.
- (9) Váhovská, L.; Bukrynov, O.; Potočňák, I.; Čížmár, E.; Kliuikov, A.; Vitushkina, S.; Dušek, M.; Herchel, R. New Cobalt(II) Field-Induced Single-Molecule Magnet and the First Example of a Cobalt(III) Complex with Tridentate Binding of a Deprotonated 4-Amino-3,5-Bis(Pyridin-2-Yl)-1,2,4-Triazole Ligand: New Cobalt(II) Field-Induced Single-Molecule Magnet and the First Example of a Cobalt(III) Complex with Tridentate Binding of a Deprotonated 4-Amino-3. *Eur. J. Inorg. Chem.* **2019**, *2019*, 250–261.
- (10) Chen, L.; Zhou, J.; Cui, H.-H.; Yuan, A.-H.; Wang, Z.; Zhang, Y.-Q.; Ouyang, Z.-W.; Song, Y. Slow Magnetic Relaxation Influenced by Change of Symmetry from Ideal Ci to D3d in Cobalt(II)-Based Single-Ion Magnets. *Dalton Trans.* **2018**, *47*, 2506–2510.
- (11) Zhang, Y.-Z.; Gómez-Coca, S.; Brown, A. J.; Saber, M. R.; Zhang, X.; Dunbar, K. R. Trigonal Antiprismatic Co(II) Single Molecule Magnets with Large Uniaxial Anisotropies: Importance of Raman and Tunneling Mechanisms. *Chem. Sci.* **2016**, *7*, 6519–6527.
- (12) Pavlov, A. A.; Savkina, S. A.; Belov, A. S.; Nelyubina, Y. V.; Efimov, N. N.; Voloshin, Y. Z.; Novikov, V. V. Trigonal Prismatic Tris-Pyridineoximate Transition Metal Complexes: A Cobalt(II) Compound with High Magnetic Anisotropy. *Inorg. Chem.* **2017**, *56*, 6943–6951.

- (13) Nemeč, I.; Herchel, R.; Trávníček, Z. Two Polymorphic Co(II) Field-Induced Single-Ion Magnets with Enormous Angular Distortion from the Ideal Octahedron. *Dalton Trans.* **2018**, *47*, 1614–1623.
- (14) Roy, S.; Oyarzabal, I.; Vallejo, J.; Cano, J.; Colacio, E.; Bauza, A.; Frontera, A.; Kirillov, A. M.; Drew, M. G. B.; Das, S. Two Polymorphic Forms of a Six-Coordinate Mononuclear Cobalt(II) Complex with Easy-Plane Anisotropy: Structural Features, Theoretical Calculations, and Field-Induced Slow Relaxation of the Magnetization. *Inorg. Chem.* **2016**, *55*, 8502–8513.
- (15) Ding, Z.-Y.; Meng, Y.-S.; Xiao, Y.; Zhang, Y.-Q.; Zhu, Y.-Y.; Gao, S. Probing the Influence of Molecular Symmetry on the Magnetic Anisotropy of Octahedral Cobalt(II) Complexes. *Inorg. Chem. Front.* **2017**, *4*, 1909–1916.
- (16) Tu, D.; Shao, D.; Yan, H.; Lu, C. A Carborane-Incorporated Mononuclear Co(II) Complex Showing Zero-Field Slow Magnetic Relaxation. *Chem. Commun.* **2016**, *52*, 14326–14329.
- (17) Vallejo, J.; Pardo, E.; Viciano-Chumillas, M.; Castro, I.; Amorós, P.; Déniz, M.; Ruiz-Pérez, C.; Yuste-Vivas, C.; Krzystek, J.; Julve, M.; et al. Reversible Solvatomagnetic Switching in a Single-Ion Magnet from an Entatic State. *Chem. Sci.* **2017**, *8*, 3694–3702.
- (18) Yang, R.-C.; Wang, D.-R.; Liu, J.-L.; Wang, Y.-F.; Lin, W.-Q.; Leng, J.-D.; Zhou, A.-J. Phosphine Oxide Ligand Based Tetrahedral Co(II) Complexes with Field-Induced Slow Magnetic Relaxation Behavior Modified by Terminal Ligands. *Chem. Asian J.* **2019**, *14*, 1467–1471.
- (19) Świtlicka, A.; Machura, B.; Kruszynski, R.; Cano, J.; Toma, L. M.; Lloret, F.; Julve, M. The Influence of Pseudohalide Ligands on the SIM Behaviour of Four-Coordinate Benzylimidazole-Containing Cobalt(II) Complexes. *Dalton Trans.* **2018**, *47*, 5831–5842.
- (20) Zhu, Y.-Y.; Liu, F.; Liu, J.-J.; Meng, Y.-S.; Jiang, S.-D.; Barra, A.-L.; Wernsdorfer, W.; Gao, S. Slow Magnetic Relaxation in Weak Easy-Plane Anisotropy: The Case of a Combined Magnetic and HFPR Study. *Inorg. Chem.* **2017**, *56*, 697–700.
- (21) Bruno, R.; Vallejo, J.; Marino, N.; De Munno, G.; Krzystek, J.; Cano, J.; Pardo, E.; Armentano, D. Cytosine Nucleobase Ligand: A Suitable Choice for Modulating Magnetic Anisotropy in Tetrahedrally Coordinated Mononuclear Co(II) Compounds. *Inorg. Chem.* **2017**, *56*, 1857–1864.
- (22) Vaidya, S.; Tewary, S.; Singh, S. K.; Langley, S. K.; Murray, K. S.; Lan, Y.; Wernsdorfer, W.; Rajaraman, G.; Shanmugam, M. What Controls the Sign and Magnitude of Magnetic Anisotropy in Tetrahedral Cobalt(II) Single-Ion Magnets? *Inorg. Chem.* **2016**, *55*, 9564–9578.
- (23) Smolko, L.; Černák, J.; Dušek, M.; Titiš, J.; Boča, R. Tetracoordinate Co(II) Complexes Containing Bathocuproine and Single Molecule Magnetism. *New J. Chem.* **2016**, *40*, 6593–6598.
- (24) Rechkemmer, Y.; Breitgoff, F. D.; van der Meer, M.; Atanasov, M.; Hakl, M.; Orlita, M.; Neugebauer, P.; Neese, F.; Sarkar, B.; van Slageren, J. A Four-Coordinate Cobalt(II) Single-Ion Magnet with Coercivity and a Very High Energy Barrier. *Nat. Commun.* **2016**, *7*, 10467.
- (25) Rajnák, C.; Packová, A.; Titiš, J.; Miklovič, J.; Moncol', J.; Boča, R. A Tetracoordinate Co(II) Single Molecule Magnet Based on Triphenylphosphine and Isothiocyanato Group. *Polyhedron* **2016**, *110*, 85–92.
- (26) Smolko, L.; Černák, J.; Dušek, M.; Miklovič, J.; Titiš, J.; Boča, R. Three Tetracoordinate Co(II) Complexes [Co(Biq)X₂] (X = Cl, Br, I) with Easy-Plane Magnetic Anisotropy as Field-Induced Single-Molecule Magnets. *Dalton Trans.* **2015**, *44*, 17565–17571.

- (27) Nemeč, I.; Herchel, R.; Trávníček, Z. Suppressing of Slow Magnetic Relaxation in Tetracoordinate Co(II) Field-Induced Single-Molecule Magnet in Hybrid Material with Ferromagnetic Barium Ferrite. *Sci. Rep.* **2015**, *5*, 10761.
- (28) Cao, D.-K.; Wei, R.-H.; Li, X.-X.; Gu, Y.-W. Multifunctional Mononuclear Bisthienylethene-Cobalt(II) Complexes: Structures, Slow Magnetic Relaxation and Photochromic Behavior. *Dalton Trans.* **2015**, *44* (12), 5755–5762.